Microcirculatory-mitochondrial resuscitation with new anti-inflammatory therapies in experimental sepsis

Attila Rutai

Ph.D. Thesis

University of Szeged - Faculty of Medicine

Doctoral School of Multidisciplinary Medical Science

Institute of Surgical Research

Szeged, Hungary

Supervisor:

József Kaszaki Ph.D.

Szeged

2021

LIST OF FULL PAPERS RELATED TO THE SUBJECT OF THE THESIS

I. **Rutai A**, Fejes R, Juhász L, Tallósy SP, Poles MZ, Földesi I, Mészáros AT, Szabó A, Boros M, Kaszaki J. Endothelin A and B Receptors: Potential Targets for Microcirculatory-Mitochondrial Therapy in Experimental Sepsis. Shock. 2020 Jul;54(1):87-95. doi: 10.1097/SHK.0000000000001414. PMID: 31318833. **IF: 2.96**

II. Juhász L, **Rutai A**, Fejes R, Tallósy SP, Poles MZ, Szabó A, Szatmári I, Fülöp F, Vécsei L, Boros M, Kaszaki J. Divergent Effects of the N-Methyl-D-Aspartate Receptor Antagonist Kynurenic Acid and the Synthetic Analog SZR-72 on Microcirculatory and Mitochondrial Dysfunction in Experimental Sepsis. Front Med (Lausanne). 2020 Nov 27;7:566582. doi: 10.3389/fmed.2020.566582. PMID: 33330526; PMCID: PMC7729001 **IF: 5.091**

III. Tallósy SP; Poles MZ; **Rutai A** ; Fejes R ; Juhász L; Burián K; Sóki J; Szabó A; Boros M; Kaszaki J. Predicting a peritonitis prognosis in preclinical sepsis: The initial microbiology determines the outcome (Scientific Reports; under review).

LIST OF ABSTRACTS RELATED TO THE SUBJECT OF THE THESIS

I. **Rutai A**, Juhász L, Fejes R, Poles MZ, Tallósy SP, Szabó A, Vécsei L, Boros M, Kaszaki J. Contribution of N-methyl-D-aspartate receptor activation to organ dysfunction and microcirculatory - mitochondrial disturbances in experimental sepsis. In: Rakonczay, Z; Kiss, L. Proceedings of the EFOP-3.6.2-16-2017-00006 (LIVE LONGER) project. Szeged, Hungary: University of Szeged 2020. 99 p. pp. 28-28.

II. **Rutai A**, Fejes R, Tallósy SP, Poles MZ, Juhász L, Mészáros AT, Boros M, Kaszaki J. Potential role of endothelin receptors in the therapy of experimental sepsis. Critical Care. 2019 23(Suppl 2): P034

III. Tallósy SP, **Rutai A**, Juhász L, Poles MZ, Burián K, Érces D, Szabó A, Boros M, Kaszaki J, Translational value of the microbial profile in experimental sepsis studies Critical Care. 2020 24 (Suppl 1) pp. 187-187. Paper: P453.

IV. Juhász L, Poles MZ, Tallósy SzP, Urbán D, **Rutai A**, Boros M, Vécsei L, Kaszaki J. Examination of NMDA receptor inhibitors on mitochondrial respiration in rat experimental polymicrobial sepsis (in Hungarian). Hungarian Surgery (Magyar Sebészet). 2017 70: 3 pp. 267-268.

V. **A Rutai**, R Fejes, SZ Tallósy, M Poles, L Juhász, A Mészáros, M Boros, J Kaszaki Potential role of endothelin receptors in the therapy of experimental sepsis Critical Care. 2019 23 : 2 p. 72 Paper: P034

VI. **Rutai A**, Fejes R, Tallósy Sz, Poles M, Juhász L, Mészáros A, Boros M, Kaszaki J. Circulatory and mitochondrial effects of endothelin receptors in an animal model of sepsis - therapeutic options (in Hungarian) Hungarian Surgery (Magyar Sebészet). 2017 70: 3 pp. 268-268.

LIST OF FULL PAPERS NOT RELATED TO THE SUBJECT OF THE THESIS

I. Bársony A, Vida N, Gajda Á, **Rutai A**, Mohácsi Á, Szabó A, Boros M, Varga G, Érces D. Methane Exhalation Can Monitor the Microcirculatory Changes of the Intestinal Mucosa in a Large Animal Model of Hemorrhage and Fluid Resuscitation. Front Med 2020 Oct 22;7:567260. doi: 10.3389/fmed.2020.567260. **IF: 5.091**

LIST OF ABSTRACTS NOT RELATED TO THE SUBJECT OF THE THESIS

I. Bársony A, Balogh B, Zentay L, Varga Z, **Rutai A**, Boros M, Varga G, Érces D. The importance of measuring exhaled methane levels in circulatory responses after haemorrhage (in Hungarian) Hungarian Surgery (Magyar Sebészet) 2019 72 : 4, 180.

II. Érces D, Bari G, Varga Z, Zentay L, **Rutai A**, Vida N, Boros M, Varga G. Effect of exogenous methane treatment on the control of renal complications following extracorporeal circulation (in Hungarian) Hungarian Surgery (Magyar Sebészet) 2019 2017 : 4 pp. 183-183. , 1 p.

III. Csákány L, Poles M, **Rutai A**, Lantos I, Endrész V, Szabó A. Relationship between inflammatory cytokine release and endothelial glycocalyx damage in clinically relevant experimental sepsis (in Hungarian) Hungarian Surgery (Magyar Sebészet). 2019 2017 72 : 4 pp. 206-206. , 1 p.

IV. **Rutai A**, Tallósy SP, Zsikai B, Poles M, Érces D, Boros M, Kaszaki J, Methane inhalation therapy in experimental sepsis Critical Care. 2020 24 : Suppl 1 pp. 210-211. Paper: P508 , 2 p.

V. **Rutai A**, Fejes R, Tallósy SP, Poles M, Juhász L, Mészáros A, Boros M, Kaszaki J. Potential role of endothelin receptors in the therapy of experimental sepsis Critical Care 2019 23 : 2 p. 72 Paper: P034

VI. Kaszaki J, **Rutai A**, Fejes R, Tallósy SzP, Poles MZ, Érces D, Boros M, Szabó A, Investigation the relationship between organ damage, microcirculatory dysfunction and reactive oxygen intermedier formation in experimental sepsis Critical Care. 2019 23 : 72 Suppl.2 Paper: P006

VII. Bari G, Szűcs Sz, Érces D, **Rutai A**, Balogh B, Bogáts G, Boros M, Varga G Effect of methane treatment on the inflammatory response following extracorporeal circulation in an experimental large animal model (in Hungarian) Cardiologia Hingarica. 2017 47 Paper: F2

LIST OF ABBREVIATIONS

ALT	alanine aminotransferase
AST	aspartate aminotransferase
CO	cardiac output
CNS	central nervous system
Cyt c	cytochrome c
DO_2	oxygen delivery
ET-1	endothelin-1
ET-R	endothelin receptor
ETS	electron transport system
ExO_2	oxygen extraction
ICU	intensive care unit
IDF	incident dark field imaging
IL-6	interleukin-6
KYNA	kynurenic acid
MAP	mean arterial pressure
MMDS	mitochondrial and microcirculatory distress syndrome
MOF	multi-organ failure
MVH	microvascular heterogeneity
NMDA-R	N-methyl-D-aspartate receptor
NO	nitric oxide
NT	nitrotyrosine
OPS	orthogonal polarization spectral imaging
OXPHOS	oxidative phosphorylation
TPR	total peripheral resistance
PPV	proportion of perfused vessels
RCR	respiratory control ratio
ROFA	rat organ failure assessment
ROX	residual oxygen consumption
SOFA	sequential (sepsis-related) organ failure assessment
SVI	stroke volume index
VO_2	oxygen consumption
XOR	xanthine oxidoreductase

CONTENTS

SUMMARY

Sepsis is a potentially life-threatening condition caused by a dysregulated host response to infection. Along with its progression, regulatory failure is frequently associated with a mismatch between oxygen delivery (DO_2), oxygen consumption (VO_2) and a deficit in oxygen extraction (ExO_2) at the cellular level. The poorly functioning microvasculature reduces delivery of oxygen to the tissue, while the mitochondrial electron transport system (ETS) is deficient, being unable to use oxygen efficiently. These processes are closely linked and ultimately lead to microcirculatory and mitochondrial distress syndrome (MMDS), which is thought to mediate end organ damage. Given this background, the major goal of this thesis was to find a novel, clinically applicable maneuver for microcirculatory recruitment and mitochondrial resuscitation to minimize the energy deficit of the organs in experimental sepsis.

In our studies Sprague Dawley rats were subjected to fecal peritonitis or a sham operation. Invasive monitoring and blood gas analysis were performed on anesthetized animals to evaluate organ dysfunctions together with intestinal capillary microperfusion and hepatic mitochondrial respiration.

In Study 1, we characterized the time course of experimental sepsis-induced changes so as to determine the most relevant time points of data and sample collections and therapeutic interventions.

In Study 2, we investigated the consequences of modulating the hypoxia-sensitive endothelin (ET) system, which plays an established role in circulatory regulation through vasoconstrictor ET_A and ET_{B2} and vasodilator ET_{B1} receptors (ET_A-R and ET_B-R). Septic animals were treated with saline or ET_A-R antagonist, ET_{B1}-R agonist or a combination therapy 22 h after sepsis induction, while oxygen dynamics, mesenteric microcirculation and hepatic mitochondrial respiration were monitored. The ET_B-R agonist countervailed the septic hypotension, while the ET_A-R antagonist maintained microcirculation and oxygen dynamics. The combined treatment was able to integrate these beneficial effects.

Study 3 focused on the effects of kynurenic acid (KYNA), a metabolite of the kynurenine pathway of tryptophan catabolism, which exhibits pleiotropic cell-protective effects under many inflammatory conditions. Septic animals were treated with saline or received KYNA or its synthetic analogue SZR-72 after 16 and 22 h of sepsis induction. It was found that treatment with SZR-72 directly modulates mitochondrial respiration, while administration of KYNA restores microcirculation.

In conclusion, our results suggest that a mixed ET receptor-targeted treatment or therapy with KYNA or the synthetic analogue SZR-72 may offer novel possibilities for a simultaneous microcirculatory and mitochondrial resuscitation strategy in sepsis. Despite compartmentalization, the microcirculatory and mitochondrial functions are closely linked under physiological circumstances. The common denominator of both mechanisms may be the capillary-mitochondrial oxygen gradient, which may be a decisive factor in mitochondrial function in sepsis. Therefore, the efficacy of microcirculatory resuscitation therapies may also be manifested at the level of subcellular oxygen consumption and energy production, and these treatment strategies could provide a novel option via influencing septic microcirculatory and mitochondrial processes.

1. INTRODUCTION

1.1 Definitions of sepsis

Sepsis is one of the oldest diseases in the history of medicine. The word *sepsis* originates from the time of Hippocrates, when it was considered a process of flesh rotting and wounds festering (Rittirsch et al. 2008). During its long history, definitions, concepts, and diagnostic and therapeutic approaches related to sepsis have changed a great deal (Esposito et al. 2017). A modern definition of sepsis was first formulated at a consensus congress in 1991 (Bone et al. 1992), which provided classifications for severe sepsis, septic shock and multiple organ dysfunction syndrome (Figure 1). It was updated in 2001 with a list of symptoms and signs to better reflect bedside experiences (Levy et al. 2003).

Later, in 2016 the Third International Consensus Definition for Sepsis and Septic Shock (Sepsis-3) consensus conference redefined the terms *inflammation*, *sepsis* and *septic shock* (Singer et al. 2016). According to this landmark definition, sepsis is a potentially life-threatening organ dysfunction caused by a dysregulated host response to an infection. Septic organ dysfunction is characterized by the sequential (sepsis-related) organ failure assessment (SOFA) scores. Septic shock is a subcategory of sepsis, which includes more severe circulatory, metabolic and cellular disorders than general sepsis, and is characterized by uncontrollable hypotension despite adequate fluid resuscitation (Singer et al. 2016) (Figure 1).

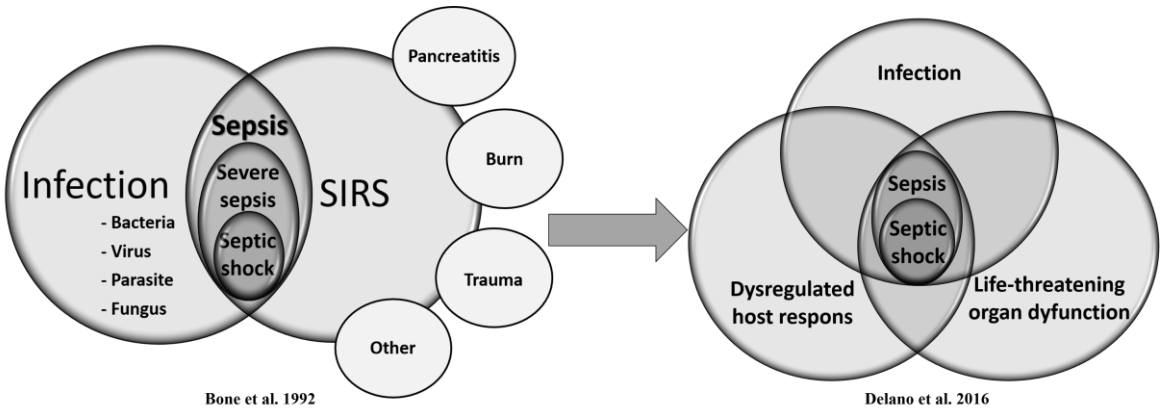

Figure 1. Changes in sepsis definition. First, sepsis was defined as systemic inflammatory response syndrome (SIRS) together with an infection, where sepsis, severe sepsis and septic shock categories were present (Bone et al. 1992; Delano et al. 2016; Singer et al. 2016).

1.2 Clinical importance of sepsis

The World Health Assembly (WHA) and World Health Organization (WHO) made sepsis a global health priority and adopted a resolution to improve prevention, diagnosis and management (Reinhart et al. 2017). According to the results of the Intensive Care Over Nations study, 29.5 % of patients had sepsis on admission to an intensive care unit (ICU) or during ICU care. Because of the complexity of sepsis-associated multiple organ failure, sepsis remains one of the greatest therapeutic challenges. In addition, the persistently high morbidity and mortality of sepsis place an enormous financial burden on healthcare. ICU mortality for patients with sepsis was 25.8%, while hospital mortality was 35.3%. These values are significantly higher than general ICU mortality rates (ICU mortality: 16.2%; hospital mortality: 24.2%) (Vincent et al. 2014). The adequate treatment of sepsis-induced multiple organ failure (MOF) is one of the most challenging tasks in ICUs (Singer et al. 2016).

1.3 Pre-clinical sepsis modeling

Experimental sepsis models can provide a good basis for the development of human therapeutics. However, an effective laboratory strategy cannot always be transferred directly to clinical practice. In this case, the lack of translational success is often attributed to incongruences between the model and human pathologies. Also in sepsis, there are several examples of divergent outcomes and conflicting results, and therefore evidence-based guidelines strengthen the value of pre-clinical testing (Lewis et al. 2016). Recently, the Minimum Quality Threshold in Preclinical Sepsis Studies (MQTiPSS) criteria outlined a recommended scheme for the design of rodent experiments (Osuchowski et al. 2018) and highlighted the importance of consecutive evaluation of established signs of organ failure, similarly to the SOFA scoring systems in human patients (Singer et al. 2016; Vincent et al. 1996). The bacterial strains of human or rat stool are broadly representative of the principally polymicrobial flora of the distal colon. Among the many alternatives to cecal ligation puncture (CLP), which is considered the gold standard, abdominal fecal slurries and injections of fecal suspensions can reduce the inherent variance of invasive surgical procedures (Dejager et al. 2011; Murando et al. 2019). Intraabdominal sepsis is a dynamic process involving potentially destructive events when the pro-inflammatory process trespasses the peritoneal cavity and extends to the circulatory system and several lines of host defense to eliminate the insult (Nemzek et al. 2008).

It is thus an important task to determine the "goodness of fit" of sepsis models. The majority of preclinical studies are performed with small animals, of which mouse and rat models are the most widely used. Considering the MQTiPSS recommendations, the mouse may be more suitable for sepsis studies as compared to the rat, mainly due to the rat's greater resistance to inflammatory insults (Osuchowski et al. 2018). However, it is important to note that, despite this limitation, the size of the rat makes it more suitable for more complex instrumentation and monitoring, as well as for taking larger volumes of blood and tissue samples, and therefore a more accurate assessment of changes is possible. In order to investigate therapeutic effects in any model in a relevant way, it is essential to investigate the dynamics of changes, i.e. the time course of responses to the applied stimulus, and to define the time window where the changes are most comparable to those observed in human sepsis. As the oxygen deficit is a key component of human sepsis, hypoxia markers and oxygen dynamics may be the most appropriate to determine the ideal monitoring/treatment window.

1.4 Pathomechanism of sepsis and septic shock

A well-balanced host response to infection is a complex process that localizes and controls the microbial invasion through the release of several pro- and anti-inflammatory mediators. Optimally, the infectious insult is overcome; however, during sepsis these pro- and anti-inflammatory processes are overturned (Rittirsch et al. 2008; Taeb et al. 2017). Over time, the uncontrolled inflammatory reactions have severe hemodynamic and oxygen dynamic consequences, leading to the development of MOF. In the first phase, infection results in excessive output of inflammatory mediators. This "cytokine storm" involves several factors such as tumor necrosis factor-α (TNF-α), interleukin-6 (IL-6) and IL-1, resulting in fever and a hypermetabolic/hyper-inflammatory condition (Chousterman et al. 2017; Piechota et al. 2007), which elevates the tissue and cellular oxygen consumption (VO_2) and oxygen extraction (ExO_2). In addition, this "cytokine storm" also stimulates nitric oxide (NO) production, leading to systemic vasodilation and a continuous decrease in total peripheral resistance (TPR).

In response to this change, compensatory mechanisms, such as elevated cardiac output (CO), tachycardia and increased oxygen delivery (DO_2), could compensate for the decrease in TPR and provide oxygen supply for the increased VO_2 (Armstrong et al. 2017).

Along with the progression of sepsis, activation of the inflammatory cascade is associated with a discrepancy between DO_2 and consumption (VO_2) in tissues, which can lead to an oxygen extraction and cellular energy deficit. In addition, despite the compensating tachycardia, CO decreases as a result of the ongoing systemic vasodilation, continuous plasma depletion due to increased vascular permeability (hypovolemia) and a reduction in cardiac contractility due to myocardial depression (Wolfárd et al. 2000). This process could lead to a hypodynamic state of sepsis, characterized by the exhaustion of compensatory mechanisms, immunoparalysis, a progressive fall in blood pressure and an increase in TPR, which may indicate severe MOF (Armstrong et al. 2017; Singer et al. 2016).

Microcirculation

The changes in oxygen dynamics at the macrocirculatory level outlined above fundamentally determine tissue and cellular oxygen transport and consumption (Arulkumaran et al. 2016; De Backer et al. 2014;). Loss of the vasodilator-vasoconstrictor balance, the decrease of adequate systemic filling pressure, and the hyper-coagulation result in insufficient microperfusion, which leads to tissue hypoxia. Moreover, the hemodynamic coherence between the macro- and microcirculation is lost; microcirculatory hypoxia can exist together with a normal systemic hemodynamic state or even in resuscitated states of shock as well (Ince et al. 2016). The poorly and abnormally functioning microvasculature result in reduced DO_2 to the tissue. Microcirculation in sepsis is mainly characterized by a decrease in perfused vessels and red blood cell velocity (RBCV) (Érces et al. 2011), along with high heterogeneity in microperfusion (Dubin et al. 2020).

Mitochondria

Inadequate microcirculation may result in a decrease in tissue and subcellular oxygen and substrate supply, which may determine mitochondrial oxygen consumption. Mitochondria are less able to drive the oxidative phosphorylation of ADP to ATP, which will lead to cellular energy deficit. Another serious consequence of mitochondrial dysfunction is increased production of reactive oxygen derivatives and the resulting direct cellular damage caused by oxidative stress (Zhang et al. 2018). As the mitochondrial electron transport system (ETS) is insufficient, it is unable to use oxygen efficiently; the energy deficit thus leads eventually to cell damage and death.

Since microcirculation and mitochondrial functions are closely interrelated under physiological conditions, their disturbance also occurs simultaneously under

pathophysiological conditions and leads to complex microcirculatory and mitochondrial distress syndrome (MMDS), which is believed to mediate the septic organ damage (Balestra et al. 2009; Pool et al. 2018; Spronk et al. 2014).

1.5 Sepsis therapies

Today, the main strategy for the management of sepsis is the use of respiratory and circulatory support therapies, including vasopressor/inotropic therapies and fluid resuscitation. The basic concept of organ-supportive therapies is therefore to increase oxygen uptake and transport, providing an adequate supply to meet subcellular oxygen demand (Armstrong et al. 2017; Balestra et al. 2009; Singer et al. 2016). Still, the currently used respiratory- and circulatory-supportive modalities cannot always improve sepsis-induced alterations at the later stages (Balestra et al. 2009; Reinhart et al. 2017).
In addition, the failing microcirculation cannot provide sufficient DO_2, and the insufficiency of the mitochondrial ETS cannot sustain the adequate aerobic metabolism of the organs (Arulkumaran et al. 2016; Balestra et al. 2009). In recent years, the bi-directional interaction between the microcirculation and mitochondria has become a focus of investigations, and it has grown increasingly apparent to date that the mechanisms involved in microcirculatory and mitochondrial dysfunction are different from those implicated in the development of macrohemodynamic changes (Balestra et al. 2009; De Backer 2014; Zhang et al. 2018). However, therapeutic opportunities to improve microcirculation and mitochondrial function are currently not available. Therefore, one of the main questions is: which therapeutic approach would be a more effective option in the treatment of sepsis?

Anti-inflammatory therapies in sepsis

In a condition with excessive immune activations, immunomodulatory, anti-inflammatory therapies are among the first therapeutic options, but they have unfortunately not been sufficiently effective so far (Eichacker et al. 2002; Freeman et al. 2000; Riedemann et al. 2003). Several anti-inflammatory therapeutics have been investigated in the past in experimental conditions, such as anti-IL-6, TNF-α and even NO synthase (NOS)-inhibiting therapies, but these strategies have not lived up to expectations (Petros et al. 1991; Qui et al. 2011; Reinhart et al. 2001; Tanaka et al. 2016). A classification of the severity and quality of the inflammatory reaction could help to determine whether the patient would benefit from immunological immunosuppression or immune activation. According to Reinhart et al., along with some beneficial effects, the most problematic part of TNF-α is that it is necessary

to identify patients who would potentially benefit from anti-inflammation. It is also suggested that the effectiveness of this therapy depends on several less-controlled factors, such as septic immune state, age, genetic disposition and even type of infection (Qui et al. 2011; Reinhart et al. 2001). Non-selective NOS inhibition has been associated with even more deleterious complications in clinical trials, where the treatment increased mortality in patients with septic shock due to adverse cardiovascular side-effects (López et al. 1998). From these previous results, it can be concluded that anti-inflammatory therapeutic approaches alone are not sufficient, as they are not necessarily able to reduce tissue and cellular hypoxia and oxygen utilization.

Vasodilator therapies

Another therapeutic option might be vasodilator manipulation of the microcirculation, which can open the shunted or closed microcirculatory units and improve the imbalance between tissue oxygen supply. Several studies have tested vasodilator therapies in experimental circumstances with different results (Boerma et al. 2010; Trzeciak et al. 2014). It has been shown that administration of nitroglycerin was not able to improve the sublingual microcirculation in patients with sepsis and septic shock (Boerma et al, 2010), and similar results have been obtained with inhaled NO administration (Trzeciak et al. 2014). Therefore, the constantly recurring concern is timing and site specificity; the ideal sepsis therapy could increase the systemic driving pressure parallel to the opening of insufficient microcirculation through vasodilation (Balestra et al. 2009; Inscho et al. 2005).

Restoring oxygen debt and energy deficits

Probably the most promising approach would be to overcome the established oxygen and energy deficits, improve tissue oxygenation and mitigate the inflammatory effects generated by hypoxic events. Based on this approach, future sepsis research should focus on improving tissue microperfusion and subcellular mitochondrial function at the same time. However, there are currently no therapeutic options for microcirculation and mitochondrial targeted resuscitation. Therefore, it is important to find new therapeutic targets, which can effectively modulate regional tissue microperfusion and subcellular oxygen consumption. The endothelin (ET) system could be such a potential target through its central regulatory role.

1.6 The endothelin system in sepsis

It has been shown that the hypoxia-sensitive ET system plays an important role in the pathophysiology of inflammatory reactions. The members of the endothelial ET family are key peptide regulators of circulation, endothelin-1 (ET-1) being the major isoform among them (Davenport et al. 2016; Yanagisawa et al. 1988). ET-1 effects are mediated by at least two types of G-protein-coupled receptors: the ET_A receptor (ET_A-R) mediates vasoconstriction, while the ET_B receptor (ET_B-R) mediates vasoconstriction (ET_{B2}-R subtype) and vasodilation (ET_{B1}-R subtype) (Brooks et al. 1995).

Previous findings have shown that elevated ET-1 levels correlate with the severity and mortality of sepsis both in animals and humans (Forni et al. 2005; Pittet et al. 1991). The ETs and ET receptors are involved in inflammatory events as well (Boros et al. 1998), and, more importantly, ET_A-R antagonist treatments have potential therapeutic benefits in experimental sepsis (Goto et al. 2010) and ischemia-reperfusion (IR)-induced microcirculatory insufficiency (Wolfárd et al. 2002). The functional role of ET_{B1}-R is less clear. However, the stimulation of ET_{B1}-R also provides tissue protection in pro-inflammatory and IR conditions in the peripheral and central nervous system (CNS) (Gulati et al. 2018), and this activity may also have relevant peripheral microcirculatory effects through an influence on the reuptake of ET-1 (Davenport et al. 2016) (Figure 2).

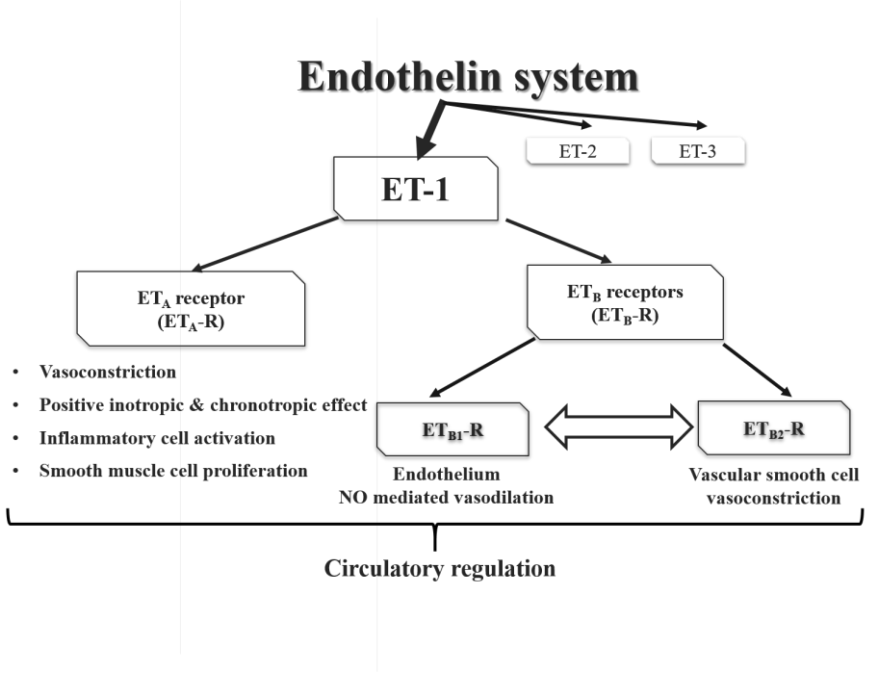

Figure 2. The endothelin system, ET-1 and the effects of receptor types

1.7 Role of the L-tryptophan–kynurenic acid system in sepsis

L-tryptophan is an essential amino acid for protein synthesis and a precursor to several bioactive molecules. The metabolites and end products of the tryptophan–L-kynurenine pathway have already been implicated in several ischemic and inflammatory disorders in the CNS (Vécsei et al. 2013). This pathway generates excitotoxic, N-methyl-D-aspartate receptor (NMDA-R) agonist quinolinic acid and the glutamate receptor antagonist kynurenic acid (KYNA) (Kiss and Vécsei 2009) (Figure 3). Further, elevated plasma KYNA levels have been reported as being associated with pro-inflammatory cytokines and increased lactate concentrations in septic shock patients (Dabrowski et al. 2014). KYNA has a high affinity for the glycine co-agonist site on NMDA-R, binds to orphan G protein-coupled receptor GPR35 and the aryl hydrocarbon receptor (Tanaka et al. 2020), and therefore takes part in the modulation of glutamatergic neurotransmission and alleviates the adaptive immune response (Walczak et al. 2020). Interestingly, sepsis-induced tissue hypoxia is also associated with activation of NMDA-R, which can lead to glutamate excitotoxicity and oxidative/nitrosative stress-mediated cell damage (Rameaut et al. 2004). KYNA is thus considered a non-receptor-specific molecule (Walczak et al. 2020); therefore, despite the properties and pleiotropic effects, the role of KYNA in the regulation of the circulatory system is still unclear.

To address this issue, several existing synthetic KYNA analogues have been tested in different models, mainly focusing on their effects on CNS. Among these, one of the most promising synthetic analogues is blood–brain barrier-permeable SZR-72 (Fülöp et al. 2009; Knyihar-Csillik et al. 2008). Inhibition of the excessive NMDA-R activation in the enteric nervous system with KYNA or its synthetic analogues has been documented in various experimental models of inflammatory bowel diseases (Érces et al. 2012; Kaszaki et al. 2012; Varga et al. 2010). Apart from neurons, the expression of receptor subunits was confirmed in peripheral organs, including the heart, small intestine, pancreas and liver (Hogan-Cann and Anderson 2016), where the activation of cellular NMDA-Rs may initiate oxidative stress, mitochondrial dysfunction and apoptosis through calcium (Ca^{2+})- and reactive oxygen species (ROS)-mediated pathways (Gingrich et al. 2004).

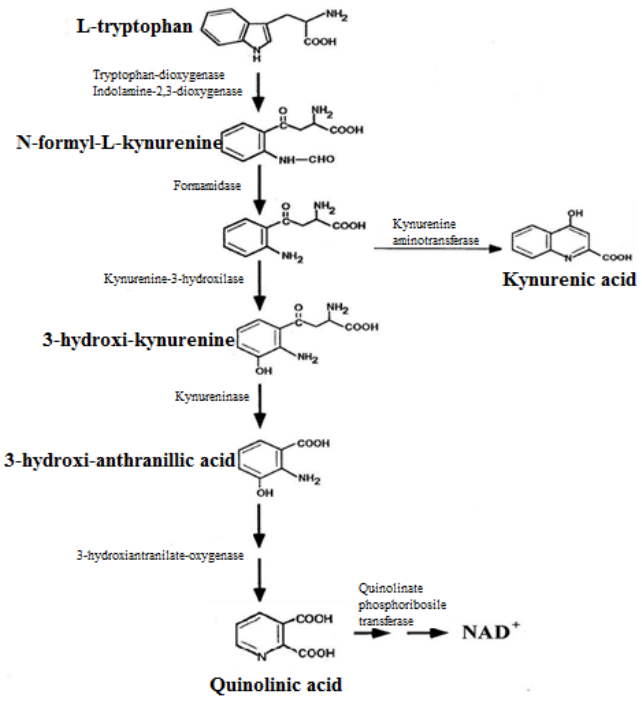

Figure 3. The L-tryptophan metabolism (Kiss and Vécsei 2005)

2. MAIN GOALS

The main goal of this thesis is to determine novel, therapeutic anti-inflammatory maneuvers, to influence the microcirculation-linked oxygen debt and to minimize the energy deficit of the organs during the septic response. Specifically, we characterized a sepsis model and tested the hypothesis that the manipulation of the ET or L-tryptophan-KYNA system might play an important role in the resuscitation of the sepsis-induced microcirculatory and mitochondrial abnormalities (MMDS) and organ failure in experimental conditions. In this context, our objectives were as follows.

- To design and characterize a novel rodent model of intraabdominal sepsis and to examine the outcome of planned therapeutic strategies. Our aim was to characterize the time course of the septic reaction in our experimental set-up to determine the optimal timing for treatment when the changes mimic the human disease.
- The modulation of ET_A-R- and ET_{B1}-R-transmitted effects may have an influence on microcirculatory recruitment and mitochondrial respiration as well. These reactions have not yet been studied in the setting of sepsis. Therefore, we wanted to examine the individual and combined effects of ET_A-R antagonism and selective ET_{B1}-R activation.
- We hypothesized that administration of KYNA and its synthetic analogue SZR-72 might be a therapeutic tool to reduce microcirculatory and mitochondrial disturbances in sepsis.

We have investigated the connection between the microcirculation and mitochondrial function and the efficacy of microcirculatory and mitochondrial-targeted resuscitation in our experimental septic model, employing clinically relevant conditions.

3. MATERIALS AND METHODS

The experiments were performed in three studies on a clinically relevant rat model of intraabdominal sepsis. In Study 1, the long-term (72 h) effects of sepsis induction were characterized to determine the clinically most relevant period of sepsis progression. In Studies 2 and 3, macro- and microcirculatory as well as mitochondrial and biochemical changes were examined in our 24-h sepsis model. In Study 2, the effects of ET_A and ET_B-R targeted treatments were measured, while the role of NMDA receptor antagonist kynurenic acid and its synthetic analogue SZR-72 were assessed in the 24 h sepsis model in Study 3.

3.1 Animals

In the experiments, male Sprague Dawley rats (350 ± 30 g; $n_{\sum}$=187) were used. The animals were housed in plastic cages (21–23°C) with a 12/12h dark-light cycle and access to standard rodent food and water *ad libitum*. The experiments were performed in accordance with National Institutes of Health guidelines on the handling and care of experimental animals and EU Directive 2010/63 for the protection of animals used for scientific purposes (approval number: V/175/2018).

3.2 Preparation of polymicrobial inoculum sepsis induction

Polymicrobial sepsis was induced with an intraperitoneally (ip)-administered fecal inoculum. Briefly, 4 g of fresh rat feces was randomly collected from healthy rats (n=4–5) and suspended in 5 mL saline. The suspension was divided into 1 mL units, completed with sterile saline to 4 mL and incubated in a water bath for 6 h at 37°C. Three mL incubated suspension was filtered and mixed in 1 mL of agarose (2%). The concentration of the microorganisms in the suspension was determined (CFU mL^{-1}) and 1.3 mL (~0.6 mg kg^{-1}) of the mixture was injected ip for sepsis induction. Septic animals were subjected to fecal peritonitis (0.6 g kg^{-1} feces ip) or a sham operation (sterile saline ip).

3.3 Wellbeing and health state monitoring in awake state

The general condition of the animals was evaluated at 6 h after the ip injections and every 12 h thereafter using a standardized scoring system in Study 1 (Osuchowski et al. 2018; Rademann et al. 2017), where a cumulative value above 6 was considered a humane endpoint for euthanasia. In Studies 2 and 3, this general condition assessment scoring system was applied 6 and 22 h after sepsis induction to assess the health status of the animals and

to characterize the progression of sepsis (see the table on the scoring system in Annex I. Supplementary Digital Content – Figure 1, http://links.lww.com/SHK/A918).

At time points of sickness assessment, all animals received 10 mL kg^{-1} crystalloid solution subcutaneously (sc; Ringerfundin, B. Braun, Hungary) to avoid dehydration and 15 µg kg^{-1} buprenorphine sc (Bupaq, Richter Pharma, Hungary) to alleviate discomfort and pain.

3.4 Anesthesia and surgical instrumentation

At the predetermined timeline after sepsis induction, the animals were anesthetized with an ip mixture of ketamine (45.7 mg kg^{-1}) and xylazine (9.12 mg kg^{-1}) to start the monitoring. The anesthetized rats were placed in a supine position on a heating pad (37°C). A tracheostomy was performed to provide spontaneous breathing, and the right jugular vein was cannulated for continuous anesthesia (ketamine 12 mg kg^{-1} h^{-1}, xylazine 2.4 mg kg^{-1} h^{-1}, and diazepam 0.576 mg kg^{-1} h^{-1}), drug treatments and infusion (Ringerfundin B. Braun; 10 mL kg h^{-1}). The left carotid artery was cannulated to record mean arterial pressure (MAP) and heart rate (HR) (SPEL Advanced Cardiosys 1.4, Experimetria Ltd., Budapest, Hungary) in all the studies.

In Study 2, a thermistor-tip catheter was also positioned into the right carotid artery to measure core temperature and cardiac output (CO) using a thermodilution technique (SPEL Advanced Cardiosys 1.4, Experimetria Ltd., Budapest, Hungary). CO was indexed for body weight, while TPR was calculated according to standard formulas ($TPR=MAP\ CO^{-1}$; $SVI=CO\ HR^{-1}$).

After an approx. 30-min surgical preparation and 30-min stabilization, hemodynamic monitoring was performed for 30–90 min (depending on the appropriate experimental protocol). At the end of hemodynamic monitoring, arterial and venous blood samples were taken for blood gas analysis (Cobas b123, Roche Ltd., Basel, Switzerland). Simplified ExO_2 was calculated from arterial and venous oxygen saturation based on a standard formula $(SaO_2 – SvO_2)/SaO_2$) in Studies 1 and 3. In Study 2, the DO_2, VO_2 and ExO_2 values were calculated based on the following formulas: $DO_2 = CO \times [(1.38 \times Hb \times SaO_2) + (0.003 \times PaO_2)]$), $VO_2 = CO \times [(1.38 \times Hb \times (SaO_2 - SvO_2)) + (0.003 \times PaO_2)]$) and $ExO_2 = DO_2\ VO_2^{-1}$. Degree of lung injury was determined by calculating the PaO_2/FiO_2 ratio (Carrico index) from partial arterial oxygen pressure (PaO_2) and FiO_2 (which was 0.21) in all the studies.

3.5 Experimental protocols

Monitoring the long-term effects of sepsis induction in Study 1

The animals were randomly assigned to sham-operated ($n_{\sum}$ = 49) and septic groups ($n_{\sum}$=51), which were randomly further divided into four independent groups each (sham-operated: n_{12h}=13, n_{24h}=12, n_{48h}=12, n_{72h}=12; septic: n_{12h}=13, n_{24h}=13, n_{48h}=13, n_{72h}=12) according to a termination timeline set between 12 and 72 h (Figure 4). Invasive monitoring was started after 12, 24, 48 and 72 h, and blood samples were taken to characterize the main components of sepsis progression (oxygen dynamics and changes in plasma ET-1 levels) as a function of time (Figure 4).

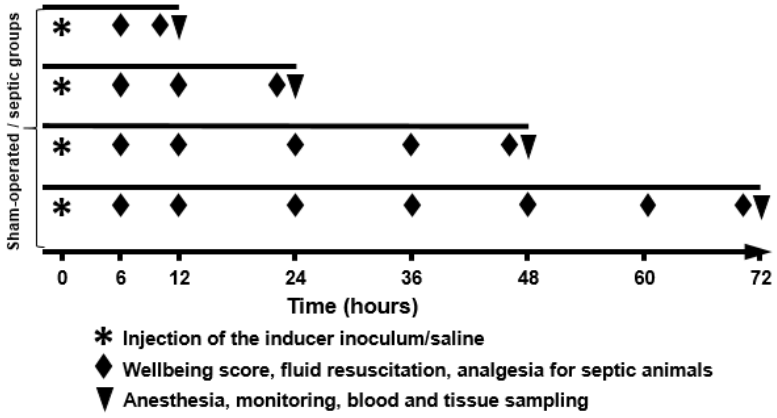

Figure 4. The experimental protocol for Study 1. The septic and sham-operated animals were randomly divided into four subgroups according to the termination timeline set: 12-24-48-72 h.

Treatment protocol and invasive monitoring in Study 2

The animals ($n_{\sum}$=55) were randomly assigned into sham-operated (Group 1, n=10) and septic (Groups 2–5, n=45) experimental groups. After a 30-min recovery period from anesthesia induction and baseline measurements, MAP, HR and CO monitoring was performed every 30 min for 90 min. Septic animals were randomly allocated to one or another of the following groups. Group 2 served as a vehicle-treated septic control and received 1 mL of saline (n=13). The next groups of septic animals received ET_A-R antagonist ETR-p1/fl peptide (100 nmol kg h^{-1}; Kurabo Ltd., Osaka, Japan; Group 3; n=11) (Baranyi et al. 1995) or the highly selective ET_{B1}-R agonist [N-Succinyl-[Glu9,Ala11,15]endothelin1] (IRL-1620; 0.55 nmol kg^{-1} h^{-1}; Sigma-Aldrich, St. Louis, MO,

USA; Group 4; n=11) (Brooks et al. 1995). Group 5 received a combination of ET_A-R antagonist and ET_{B1}-R agonist compounds in the same doses (n=10). All treatments were administered in a continuous 60-min iv infusion in 1 mL volume (Figure 5).

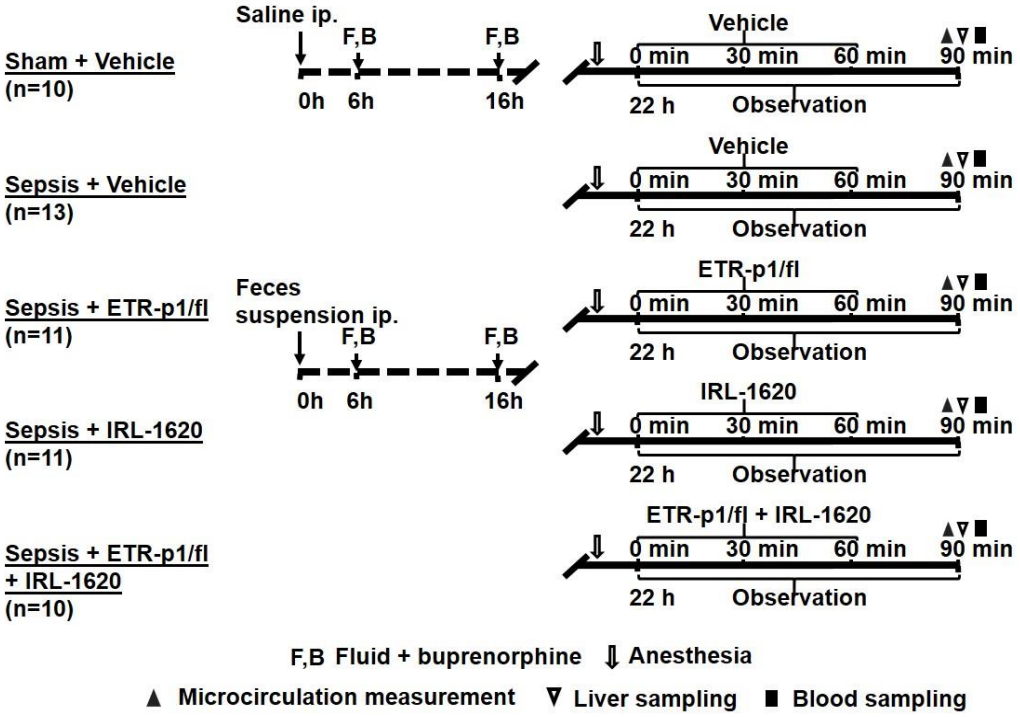

Figure 5. The experimental protocol for Study 2. The animals were randomly assigned to sham-operated and septic experimental groups. Twenty-two hours after sepsis induction, the animals were divided into four subgroups: treated with saline, ETA receptor antagonist ETR-p1/fl peptide (100 nmol kg^{-1} h^{-1} iv), ET_{B1} receptor agonist IRL-1620 (0.55 nmol kg^{-1} h^{-1} iv) or the same doses as those of the combination therapy.

Treatment protocol and invasive monitoring in Study 3

Animals (n_{Σ}=32) were randomly divided into sham-operated (n=8) and sepsis (n=24) groups. Septic animals were divided further into KYNA- (Sigma-Aldrich Inc., St. Louis, Mo., USA; 160 μmol kg^{-1} ip; n=8) or SZR-72- (2-(2-N,N-dimethylaminoethyl-amine-1-carbonyl)-1H-quinolin-4-one hydrochloride, synthesized by the Institute of Pharmaceutical Chemistry, University of Szeged, Hungary; 160 μmol kg^{-1} ip; n=8) treated and vehicle-treated control (saline ip; n=8) groups. Treatments were performed in two steps (80 μmol kg^{-1}; in 1 mL kg^{-1} saline each) 16 h and 22 h after sepsis induction. After surgery and a 30-

min stabilization, MAP and HR monitoring was performed every 15 min for a 60-min observation period (Figure 6).

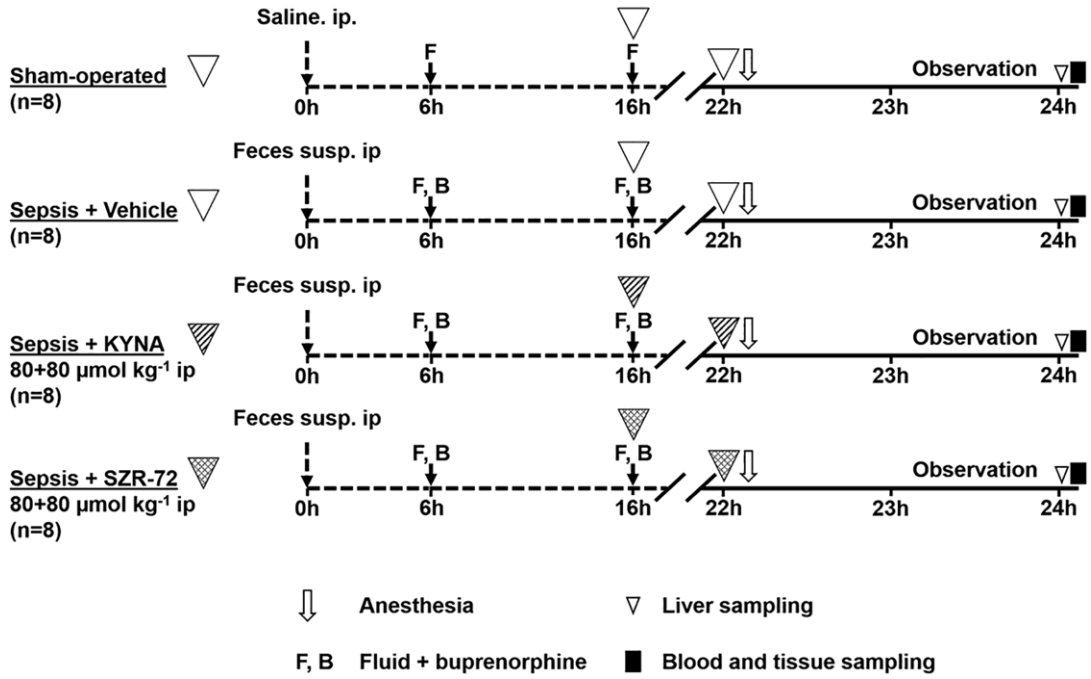

Figure 6. The experimental protocol of Study 3. The animals were randomly assigned into the sham-operated and sepsis groups. Sixteen hours after sepsis induction, animals were randomly divided into three subgroups: treated with vehicle, KYNA (80 + 80 µmol kg^{-1} ip) or SZR-72 (80 + 80 µmol kg^{-1} ip).

3.6 Microcirculatory measurements

After the observation period, a median laparotomy was performed to monitor the microcirculation of the ileal serosa using the intravital video microscope imaging technique. Microcirculatory measurements were carried out with the orthogonal polarization spectral imaging technique (OPS; Cytoscan A/R, Cytometrics, Philadelphia, PA) in Study 2, while incident dark field (IDF; CytoCam Video Microscope System; Braedius Medical, Huizen, the Netherlands) imaging techniques were used in Study 3. These contrast agent-free techniques illuminate the organ surface with linearly polarized light, where specially filtered light was reflected from the tissues and visualized by a computer-controlled sensor. The images outline the hemoglobin-containing structures, such as the microvessels, at approximately 2–300 mm of tissue depth. IDF is a newer version of OPS imaging, which

already has higher resolution and automatic data analysis and is used for bedside monitoring of the microcirculation of critically ill patients (Aykut et al. 2015; Dubin et al. 2020).

In Study 2, an empty ileum segment was placed on a specially designed stage, and serosal microcirculatory images (made by OPS technique) were recorded with an S-VHS video recorder 1 (Panasonic AG-TL 700, Matsushita Electric Ind. Co. Ltd., Osaka, Japan). A quantitative assessment of the microcirculatory parameters was performed offline by frame-to-frame blinded analysis of the videotaped images. Changes in red blood cell velocity (RBCV) and capillary perfusion rate (CPR; perfused/non-perfused area) in the serosal capillaries were determined in three separate fields with a computer-assisted image analysis system (IVM Pictron, Budapest, Hungary).

In Study 3, images (made using the IDF technique) from an ileum segment were recorded in six, 50-frame-long, high-quality video clips (spatial resolution 14 megapixels; temporal resolution 60 fps). The video was recorded at separate locations of the terminal ileum by the same investigator. The records were saved as digital AVI-DV files to a hard drive and analyzed with an offline software-assisted system (AVA 3.0, Automated Vascular Analysis, Academic Medical Center, University of Amsterdam). The screens recorded with the IDF imaging technique were divided into four equal quadrants, as recommended. The proportion of perfused vessels (PPV) was defined as the ratio of the perfused vessel lengths to total vessel lengths. The PPV values were calculated in all quadrants, and the software (Automated Vascular Analysis 3.0) for the device provided four individual PPV values, Q1 PPV, Q2 PPV, Q3 PPV and Q4 PPV. The average of these individual values (Q1PPV–Q4PPV) is shown as % PPV in the illustrations. The median PPV values for the four quadrants were used as a reference (median values for Q1–4) in calculating microvascular heterogeneity (MVH). Heterogeneity was defined as the average difference of the PPV values (%) between each quadrant and the reference value (the differences are given in absolute values) for each record using the following formula:

$$\boldsymbol{MVH} = [(\boldsymbol{M}_{\sum \mathbf{QPPV}} - \boldsymbol{Q1PPV}) + (\boldsymbol{M}_{\sum \mathbf{QPPV}} - \boldsymbol{Q2PPV}) + (\boldsymbol{M}_{\sum \mathbf{QPPV}} - \boldsymbol{Q3PPV}) + (\boldsymbol{M}_{\sum \mathbf{QPPV}} - \boldsymbol{Q4PPV})]/\text{number of quadrants}$$

M = median

$\mathbf{M}_{\sum \mathbf{QPPV}}$ = median of the summed PPV from the four quadrants

QxPPV = PPV value of an individual quadrant

This calculation provides numerical values for perfusion heterogeneity (Corrêa et al. 2017; Trzeciak et al. 2014).

3.7 Final blood and tissue samplings

After the intestinal microcirculatory measurements, a liver tissue biopsy was taken to evaluate mitochondrial respiratory functions. Tissue samples from the terminal ileum were harvested for biochemical measurements (see below). Blood samples were taken from the inferior caval vein and placed into precooled, EDTA-containing tubes (1 mg mL^{-1}) centrifuged (1200 g at 4°C for 10 min), and plasma was stored at -70°C until assay. After tissue samplings, animals were sacrificed under deep anesthesia (overdose with sodium pentobarbital 120 mg kg^{-1} iv).

3.8 Measurements of metabolic, inflammatory and organ function-related markers

Whole blood lactate levels were measured from venous blood samples (Accutrend Plus Kit, Roche Diagnostics Ltd., Rotkreuz, Switzerland) to determine metabolic imbalance.

Plasma ET-1 and IL-6 levels were determined with standard ELISA kits (Biomedica Ltd., Vienna, Austria, and Cusabio Biotechnology Ltd., Wuhan, China, respectively) following manufacturer's instructions.

Kidney injury was determined from plasma urea level, whereas liver dysfunction was assessed by measuring plasma alanine aminotransferase (ALT) levels, using a Roche/Hitachi 917 analyzer (F. Hoffmann-La Roche AG, Switzerland). All analyses were performed on coded samples in a blinded fashion.

3.9 Rat organ failure score assessment

The severity of organ failure was determined by using a scoring system adapted for rats (rat organ failure assessment – ROFA) considering the principles of the Sepsis-3 international consensus (Table 1). ROFA components were scored between 0 and 4 based on threshold values of different parameters (Zhai et al. 2018). The cardiovascular (MAP values) and respiratory components (the PaO_2/FiO_2 ratio) of ROFA were determined from readings of hemodynamic and blood gas monitoring, respectively. Sepsis-induced liver damage was determined by measuring plasma ALT level. Renal dysfunction was characterized by determining plasma urea levels. The ROFA scoring system was supplemented by scoring the degree of blood lactate level (indicative of metabolic disturbances caused by tissue

hypoxia). The ROFA values were calculated by summing up the scores in each element of the scoring system. Septic state was defined as ROFA score above 2.

Rat organ failure assessment (ROFA) score					
ROFA score:	**0**	**1**	**2**	**3**	**4**
Respiration PaO_2/FiO_2	≥400	<400	<300	<200	<100
Cardiovascular MAP (mmHg)	≥75	65<75	60<65	<60	-
Renal Plasma Urea (mg dL^{-1})	<15	7.5–21	>21	-	-
Liver ALT (U L^{-1})	<1.7	1.7–2	>2	-	-
Metabolism Lactate level (mM L^{-1})	<2	2–3	3–4	4–5	>5

Table 1. Threshold values of the rat organ failure assessment (ROFA) scoring system for the individual organ dysfunction parameters. ROFA, rat organ failure assessment; MAP, mean arterial pressure; ALT, alanine aminotransferase; AST, aspartate aminotransferase.

3.10 Evaluation of ileal xanthine oxidoreductase activity and nitrotyrosine levels

In Study 3, the same snap frozen tissues were used for these measurements. Ileum biopsies kept on ice were homogenized with a rotor stator homogenizer in a phosphate buffer (pH 7.4) containing 50 mmol l^{-1} Tris–HCl, 0.1 mmol l^{-1} EDTA, 0.5 mmol l^{-1} dithiothreitol, 1 mmol l^{-1} phenylmethylsulfonyl fluoride, 10 μg ml^{-1} soybean trypsin inhibitor and 10 μg ml^{-1} leupeptin. Homogenates were then centrifuged at 4°C for 10 min at 15,000 g, and the supernatant was then divided into one ultra-filtered part and one unfiltered one, which were used for xanthine oxidoreductase (XOR) activity and nitrotyrosine determination, respectively. XOR activity was measured in the ultra-filtered supernatant (Amicon Ultra-0.5 Centrifugal Filter) with a fluorometric kinetic assay on the basis of the conversion of pterin to isoxanthopterin in the presence (total XOR) or absence (xanthine oxidase activity) of the electron acceptor methylene blue (Beckman et al. 1989). XOR activity was calculated and expressed in μmol min^{-1} mg $protein^{-1}$. Free nitrotyrosine as a marker of peroxynitrite generation was measured from unfiltered supernatant by enzyme-linked immunosorbent

assay (Cayman Chemical, Ann Arbor, MI, USA). The supernatants were incubated overnight with antinitrotyrosine rabbit IgG and nitrotyrosine acetylcholinesterase tracer in precoated (mouse anti-rabbit IgG) microplates, followed by development with Ellman's reagent and measured spectrophotometrically at 405 and 420 nm. Tissue nitrotyrosine content was calculated in ng mg^{-1} protein. Protein content was assessed by Lowry's method.

3.11 Assessment of mitochondrial respiratory function in liver homogenates

In Studies 2–3, liver samples obtained from the left lateral lobe were washed in phosphate-buffered saline and then homogenized in a medium containing 250 mM sucrose, 0.5 mM Na_2EDTA, 10 mM Tris and 1 g L^{-1} bovine serum albumin. After homogenization, mitochondrial respiratory oxygen flux ($J_{V,O2}$; pmol $sec^{-1}mL^{-1}$) normalized to 8 mg wet weight was assessed using high-resolution respirometry (O2k, Oroboros Instruments, Innsbruck, Austria). All the measurements were performed in an MiR05 respiration medium (pH 7.1) under continuous stirring at 37°C (Doerrier et al. 2018). After a stable basal respiration (without exogenous substrates and ADP), NADH- and succinate-supported LEAK respiration and complex I (CI)- and complex II (CII)-linked capacities of oxidative phosphorylation (OXPHOS I and OXPHOS II) were determined in the presence of substrates (complex I-linked: 10 mM glutamate, 2 mM malate; and complex II: 10 mM succinate) and saturating concentration of ADP (2.5 mM). Rotenone (0.5 μM), an inhibitor of CI, was administered prior to the addition of succinate to block mitochondrial ROS production via reverse electron transport. Following stimulation of OXPHOS, the integrity of the outer mitochondrial membrane was evaluated with exogenous cytochrome c (cyt c; 10 μM). ATP synthase was blocked by oligomycin (2.5 μM) to assess LEAK respiration in a non-phosphorylating state ($LEAK_{Omy}$). The respiratory control ratio (RCR), an index of coupling between respiration and phosphorylation, was expressed as a ratio of OXPHOS to a $LEAK_{Omy}$ state. The ETS-independent respiration (or residual oxygen consumption; ROX) was determined following complex III inhibition with antimycin A (2.5 μM). DatLab 5.1 software (Oroboros Instruments, Innsbruck, Austria) was used for online display, respirometry data acquisition and analysis.

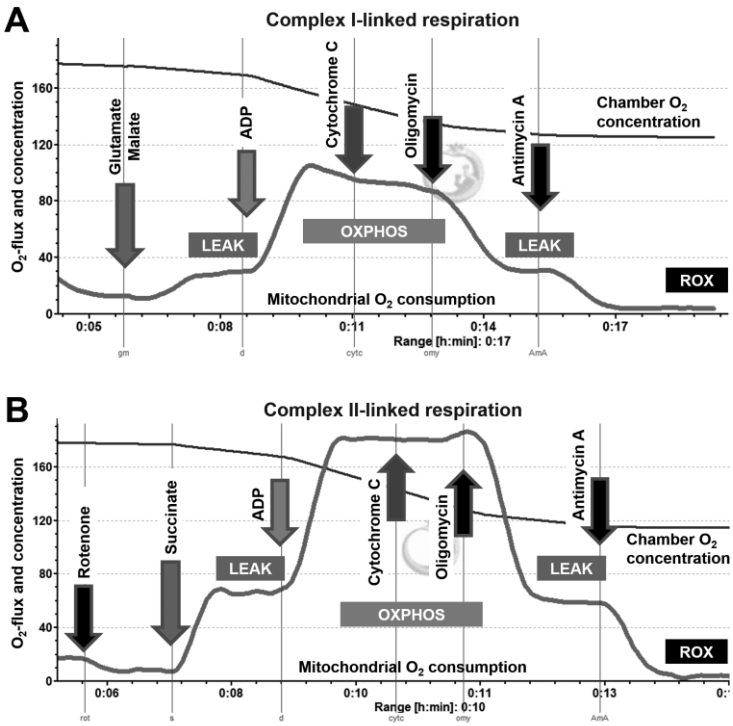

Figure 7. FluoRespirometric protocols. Complex I- and II-linked respiration, oxidative phosphorylation (OXPHOS) capacities (A, B) were assessed in energized liver homogenates. Mitochondrial electron transport system-dependent O_2 consumption was confirmed by blocking complex III with antimycin A (ROX; residual oxygen consumption).

3.12 Statistical analysis

Data analysis was performed with a statistical software package (SigmaStat for Windows, Jandel Scientific, Erkrath, Germany). Normality of data distribution was analyzed with the Shapiro–Wilk test. The Friedman analysis of variance on ranks was used within groups. Time-dependent differences from the baseline for each group were assessed with Dunn's method. Differences between groups were analyzed with the Kruskal–Wallis one-way analysis of variance on ranks, followed by Dunn's method. Median values and 75^{th} and 25^{th} percentiles are provided in the figures; *P* values <0.05 were considered significant.

4. RESULTS

Study 1

4.1 Long-term changes in plasma endothelin-1 levels and oxygen extraction

There were no significant changes in the ExO_2 between the sham-operated and septic animals at 12 h. In contrast, ExO_2 values for the septic animals started to decrease 24 h after the septic insult. In the 48th and 72nd hours, ExO_2 remained at a lower level in the septic animals, indicating that the oxygen delivery did not completely meet the tissue oxygen demand, although this decrease was not significant at these later time points (Figure 8A). Plasma ET-1 concentration was significantly elevated 24 h after sepsis induction (Figure 8B).

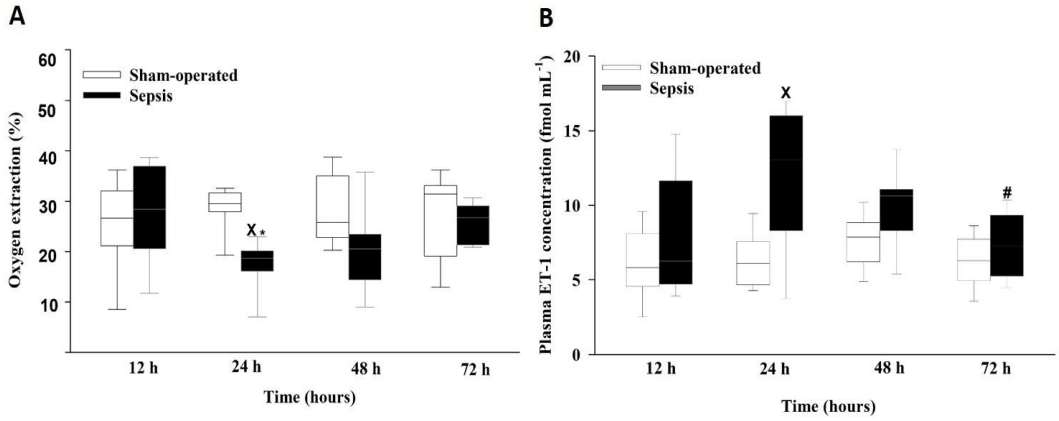

Figure 8. Time-dependent changes in oxygen extraction (A) and plasma endothelin-1 concentration (B), which are indicators of tissue hypoxia. White boxes represent the sham-operated group over time, while gray boxes represent the septic groups. The plots demonstrate the median (horizontal line in the box) and the 25th (lower whisker) and 75th (upper whisker) percentiles. Between groups: Kruskal–Wallis test and Dunn's post-hoc test. *P<0.05 sepsis vs. sham-operated.

Study 2

4.2 Changes in well-being scores

Well-being scores similarly increased in all septic groups, with no significant difference between septic groups. Score values were significantly elevated compared to those for the sham-operated group 22 h after induction in all septic groups.

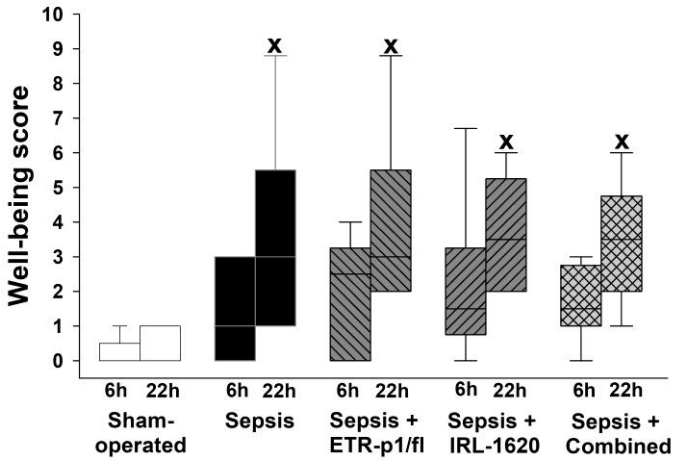

Figure 9. Changes in well-being score 6 and 22 h after sepsis induction in the different septic groups treated with saline (black box), ET_A receptor antagonist ETR-p1/fl (striped box), ET_{B1} receptor agonist IRL-1620 (striped box) and a combination of them (checked box). The plots demonstrate the median (horizontal line in the box) and the 25th (lower whisker) and 75th (upper whisker) percentiles. Between groups: Kruskal–Wallis test and Dunn's post-hoc test. $^{x}P<0.05$ vs. sham-operated; $^{\#}P<0.05$ vs. vehicle-treated sepsis.

4.3 Hemodynamic changes

In the sham-operated group, there were no significant hemodynamic changes during the observation period. Sepsis, however, was accompanied by a significant hypotension, an increase in CO and a decrease in TPR (Figure 10A, C, D). As compared to the vehicle-treated septic group, ETR-p1/fl treatment had no effect on hemodynamics, but IRL-1620 significantly increased the MAP and TPR and decreased CO and SVI during the 90-min observation period. The combined ET_A-R antagonism and ET_{B1}-R agonism caused significant increases in MAP and TPR values as compared to the baseline and to the respective values for the vehicle-treated sepsis group (Figure 10).

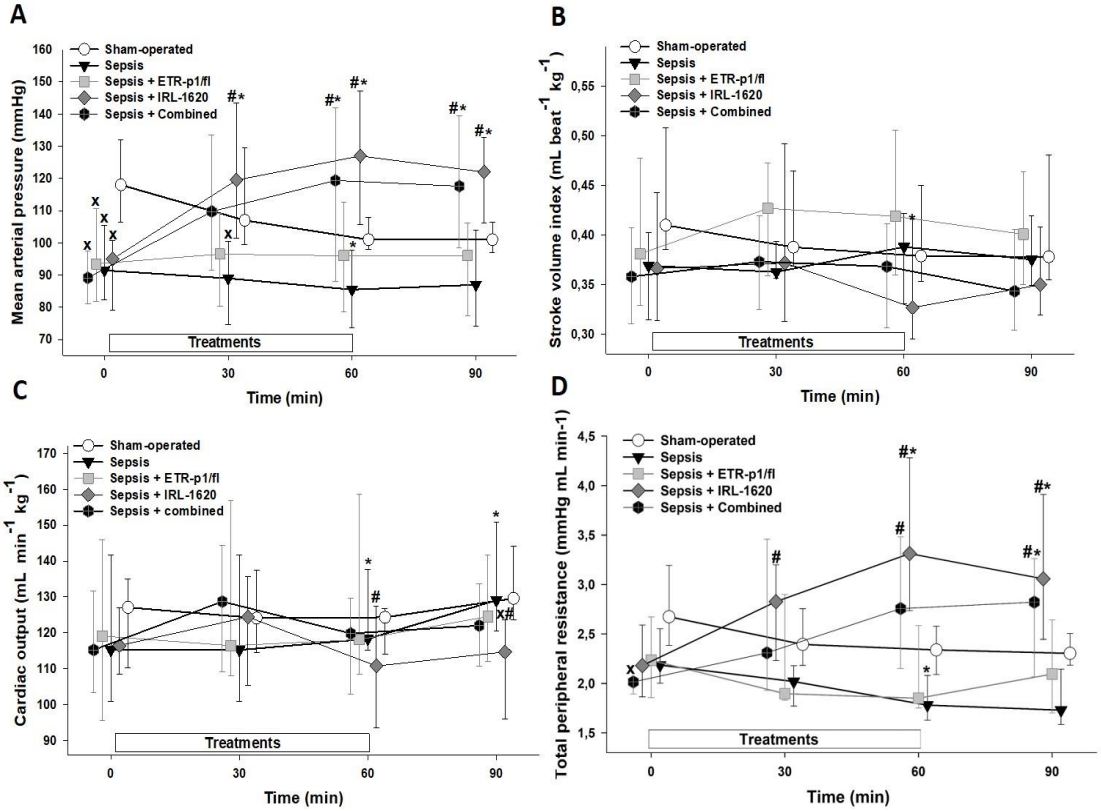

Figure 10. Changes in mean arterial pressure (A), stroke volume index (B), cardiac output (C) and total peripheral resistance response (D) in the sham-operated group (open circles) and in the different sepsis groups treated with saline vehicle (black triangle), ET_A receptor antagonist ETR-p1/fl (grey square), ET_{B1} receptor agonist IRL-1620 (grey diamond) and a combination of them (black hexagon with plus sign). The plots demonstrate the median values and the 25th (lower whisker) and 75th (upper whisker) percentiles. $^{x}P<0.05$ vs. sham operated; $^{\#}P<0.05$ vs. vehicle-treated sepsis; $^{*}P<0.05$ vs. 0-min.

4.4 Changes in oxygen dynamics

The 24-h septic period caused significant changes in oxygen dynamics, including an increase in DO_2 (Figure 11A), deterioration of VO_2, and reduced ExO_2 values and PaO_2/FiO_2 ratio (Figure 11B–C) as compared to the sham-operated group. Lung injury, characterized by the PaO_2/FiO_2 ratio, was significantly lower in the septic animals, and the ETR-p1/fl treatment or IRL-1620 treatment did not influence this change (Figure 11D). VO_2 and ExO_2 were significantly higher after ETR-p1/fl treatment as compared to the non-treated sepsis group. A significant increase in ExO_2 was observed in response to IRL-1620 treatment compared to that of the vehicle-treated sepsis group. When these treatments were

combined, the oxygen dynamic parameters were not significantly different from those of the sham-operated group, and there was a statistically non-significant trend of improvement as compared to the non-treated sepsis group (Figure 11).

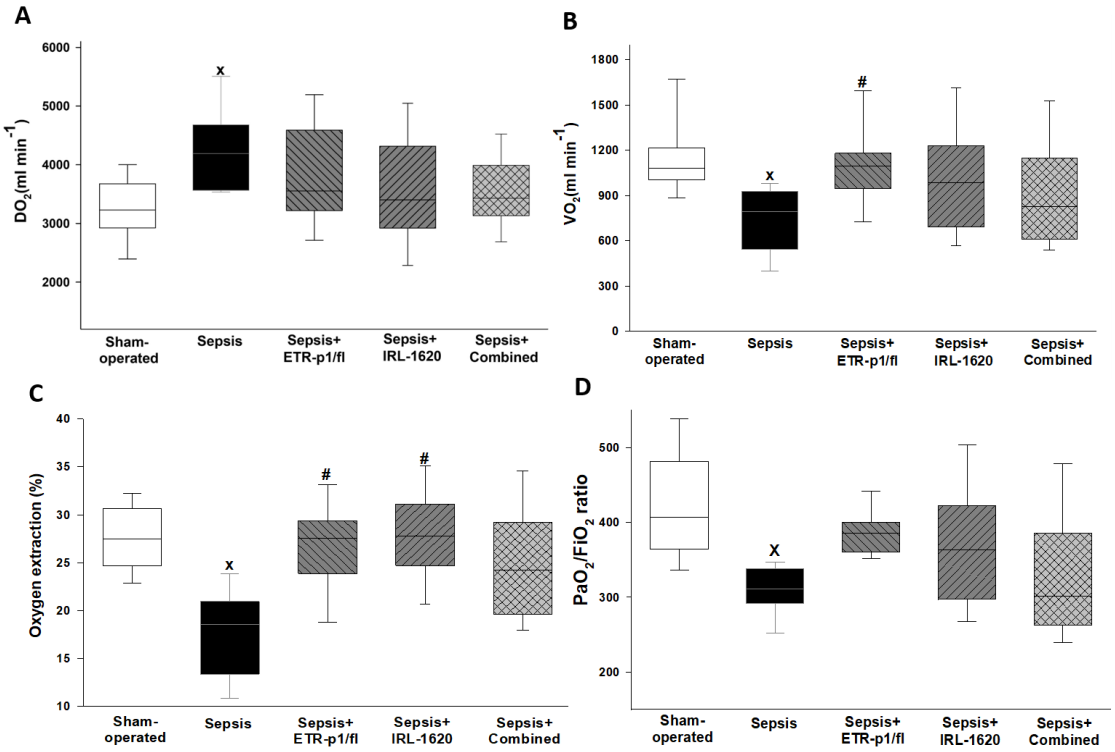

Figure 11. Oxygen delivery (DO2) (A), oxygen consumption (VO2) (B), oxygen extraction (C) and PaO_2/FiO_2 ratio (D) in the sham-operated group (empty box) and in the different septic groups treated with saline (black box), ET_A receptor antagonist ETR-p1/fl (striped box), ET_{B1} receptor agonist IRL-1620 (striped box) and a combination of them (checked box). The plots demonstrate the median (horizontal line in the box) and the 25th (lower whisker) and 75th (upper whisker) percentiles. Between groups: Kruskal–Wallis test and Dunn's post-hoc test. $^{x}P<0.05$ vs. sham-operated; $^{\#}P<0.05$ vs. vehicle-treated sepsis.

4.5 Metabolic changes and organ dysfunctions

Plasma ALT activity and urea levels were significantly higher in the non-treated septic group as compared to the sham-operated animals (Figure 12A–B). The ETR-p1/fl treatment or IRL-1620 treatment did not influence the sepsis-induced changes in plasma ALT or urea levels (Figure 12A–B). However, when the ET_A-R antagonists and ET_{B1}-R agonists were combined, the plasma ALT level was significantly lower than in the vehicle-treated septic group (Figure 12A). Similar changes were observed in AST levels (data not shown).

Likewise, polymicrobial sepsis was associated with significantly increased lactate levels in the saline-treated sepsis group. In response to the ETR-p1/fl and combined treatments, the lactate values were not different from those of the sham-operated group (Figure 12C).

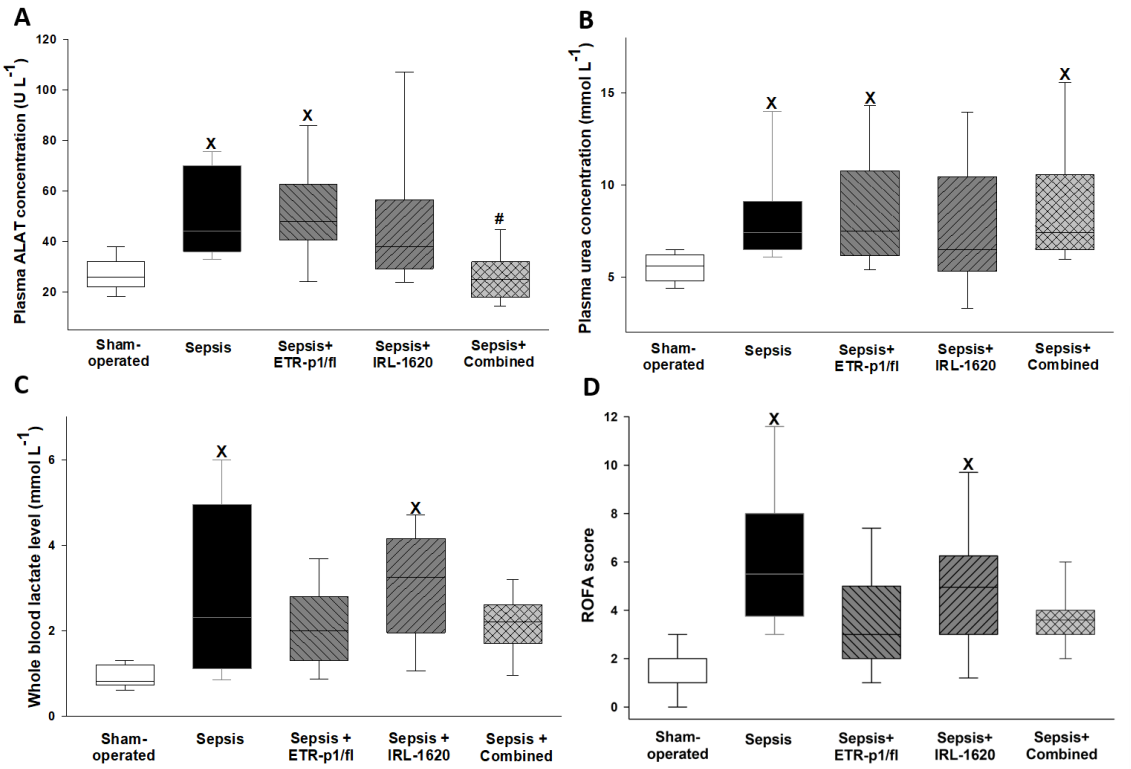

Figure 12. Plasma alanine aminotransferase (ALT) (A), urea (B), lactate levels (C) and ROFA score values (D) in the sham-operated group (empty box) and in the different sepsis groups treated with saline vehicle (black box), ET_A receptor antagonist ETR-p1/fl (striped box), ET_{B1} receptor agonist IRL-1620 (striped box) and a combination of them (checked box). The plots demonstrate the median (horizontal line in the box) and the 25th (lower whisker) and 75th (upper whisker) percentiles. $^{x}P<0.05$ vs. sham-operated; $^{\#}P<0.05$ vs. vehicle-treated sepsis.

4.6 Microcirculatory changes

The 24-h septic insult caused significant microcirculatory deterioration in the intestinal serosa. The CPR reached 55%, while RBCV was approx. 60% lower than those in the sham-operated animals (Figure 13A–B). When compared to the vehicle-treated sepsis group, ETR-p1/fl therapy caused a significant improvement in CPR, but not in RBCV. Agonism of ET_{B1}-R with IRL-1620 caused a slight, non-significant perfusion recovery without affecting changes in RBCV. A combination of the ETR-p1/fl and IRL-1620 treatments, however, was effective in restoring both parameters of the intestinal microcirculation (Figure 13A–B).

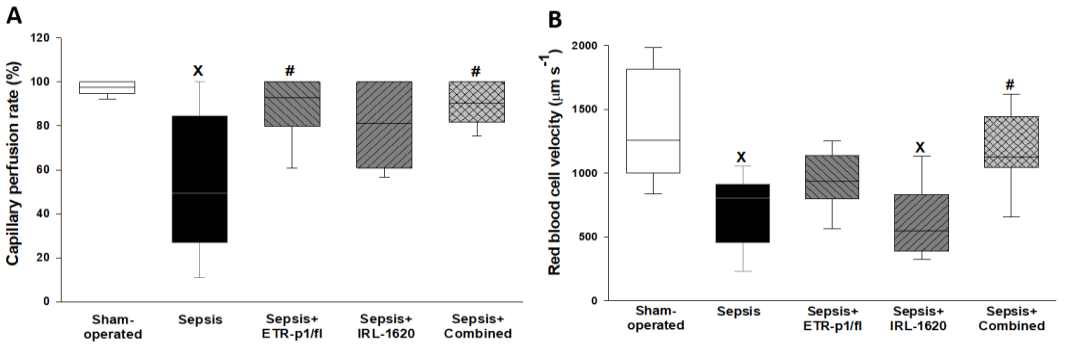

Figure 13. Capillary perfusion rate (A) and red blood cell velocity (B) in the sham-operated group (empty box) and in the different sepsis groups treated with saline vehicle (black box), ET_A receptor antagonist ETR-p1/fl (striped box), ET_{B1} receptor agonist IRL-1620 (striped box) and a combination of them (checked box). The plots demonstrate the median (horizontal line in the box) and the 25th (lower whisker) and 75th (upper whisker) percentiles. Between groups: Kruskal–Wallis test and Dunn's post-hoc test. $^{x}P<0.05$ vs. sham-operated; $^{\#}P<0.05$ vs. vehicle-treated sepsis.

4.7 Changes in inflammatory markers

In the case of sepsis, plasma IL-6 and ET-1 levels reached higher values compared to those of the sham-operated group (Figure 14A–B). IRL-1620 did not influence the sepsis-induced elevations in IL-6 and ET-1, but ETR-p1/fl treatment caused a significant reduction in plasma ET-1 level. The combined therapy significantly reduced the sepsis-induced elevation in plasma ET-1 and reduced IL-6 values as well (P=0.051).

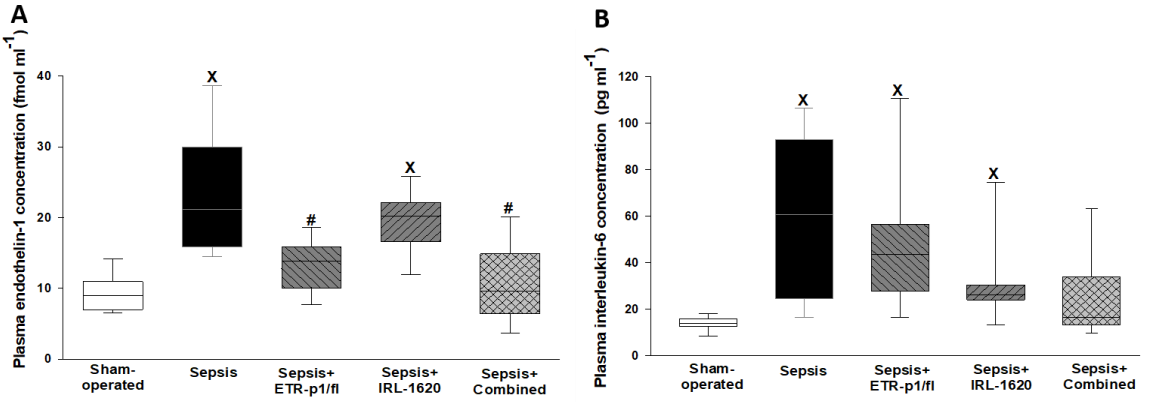

Figure 14. Plasma interleukin-6 (IL-6) concentration (A) and plasma endothelin-1 (ET-1) (B) in the sham-operated group (empty box) and in the different sepsis groups treated with saline vehicle (black box), ET_A receptor antagonist ETR-p1/fl (striped box), ET_{B1} receptor agonist IRL-1620 (striped box) and a combination of them (checked box). The plots demonstrate the median (horizontal line in the box) and the 25th (lower whisker) and 75th (upper whisker) percentiles. Between groups: Kruskal–Wallis test and Dunn's post-hoc test. $^{x}P<0.05$ vs. sham-operated; $^{\#}P<0.05$ vs. vehicle-treated sepsis.

4.8 Changes in mitochondrial respiration

Intra-abdominal sepsis significantly decreased substrate oxidation as compared to the sham operation. In comparison with the vehicle-treated sepsis group, the ET_A-R antagonist and ET_B-R agonist therapies resulted in an increasing tendency in $J_{V,O2}$, and this change was statistically significant after the combination of therapies (data not shown). As a result of septic insult, both OXPHOS capacity and RCR values were significantly lower than in the sham-operated animals (Figure 15). In comparison with the non-treated sepsis group, ETR-p1/fl treatment preserved both CII RCR and CII-linked OXPHOS values (Figure 15B–D), and an increasing trend was observed in CI-linked respiration (Figure 15C). Treatment with IRL-1620 resulted in a slight, non-significant amelioration in CI- and CII-linked OXPHOS capacity. In response to the combined treatment, CI- and CII-linked OXPHOS as well as RCR values were significantly increased (Figure 15).

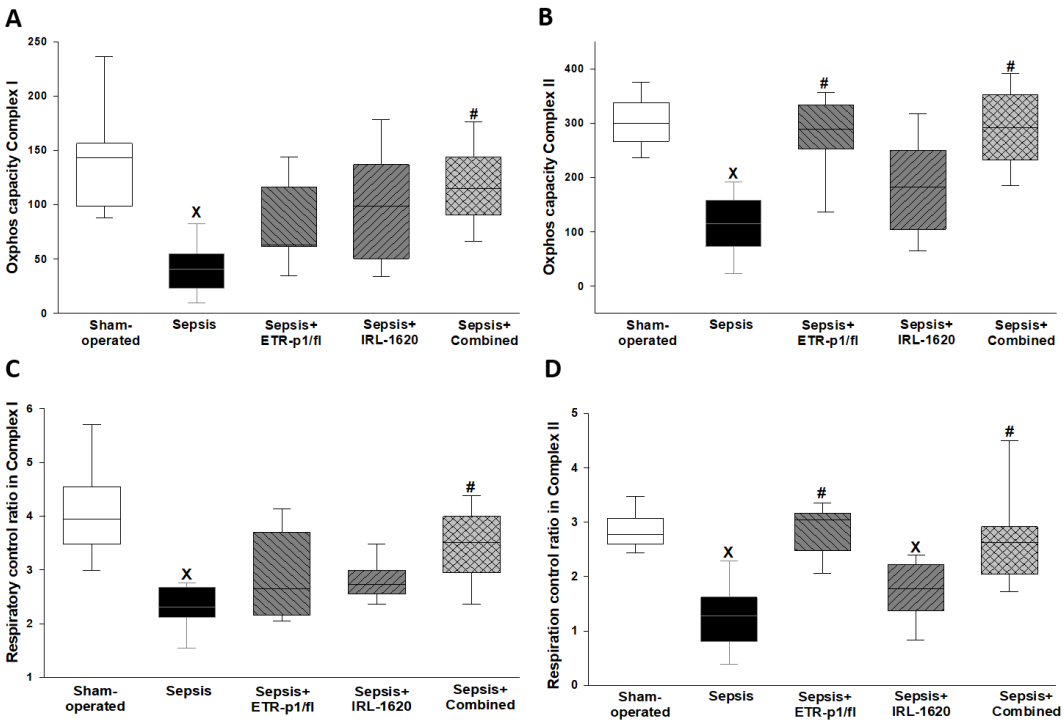

Figure 15. Complex I-linked OXPHOS capacity (C1-OXPHOS) (A), complex II-linked OXPHOS capacity (C1I-OXPHOS) (B), complex I respiration control ratio (CI-RCR) (C), and complex II respiration control ratio (CII-RCR) (D) in the sham-operated group (empty box) and in the different sepsis groups treated with saline vehicle (black box), ET_A receptor antagonist ETR-p1/fl (striped box), ET_{B1} receptor agonist IRL-1620 (striped box), and a combination of them (checked box). The plots demonstrate the median (horizontal line in the box) and the 25th (lower whisker) and 75th (upper whisker) percentiles. $^{x}P<0.05$ vs. sham-operated; $^{\#}P<0.05$ vs. vehicle-treated sepsis.

4.9 Changes in mitochondrial membrane integrity

Sepsis resulted in significant disintegration of the outer membrane based on the effect of exogenous cyt c, but preserved membrane integrity was observed in the animals subjected to the combined treatment (Figure 16A–B)

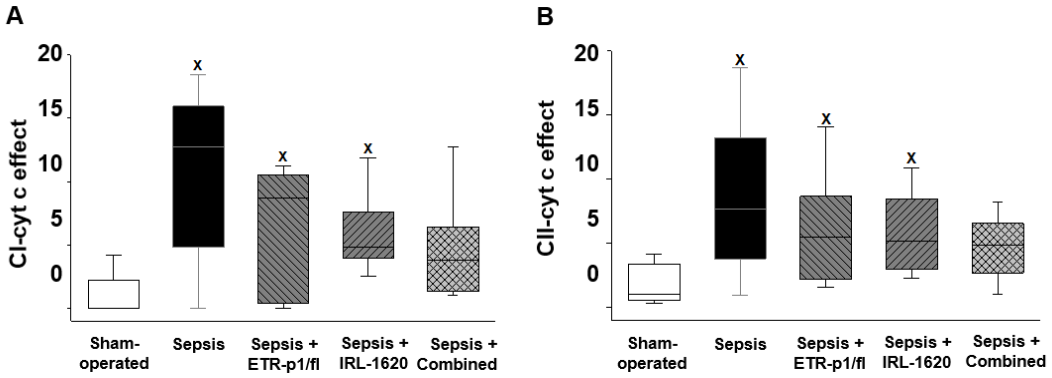

Figure 16. Complex I-linked membrane integrity (CI-cyt c) (A), complex II-linked membrane integrity in the sham-operated group (empty box) and in the different sepsis groups treated with saline vehicle (black box), ET_A receptor antagonist ETR-p1/fl (striped box), ET_{B1} receptor agonist IRL-1620 (striped box) and a combination of them (checked box). The plots demonstrate the median (horizontal line in the box) and the 25th (lower whisker) and 75th (upper whisker) percentiles. $^{x}P<0.05$ vs. sham-operated; $^{\#}P<0.05$ vs. vehicle-treated sepsis.

Study 3

4.10 Changes in well-being scores

Well-being score values did not change for the sham-operated group, while they significantly increased in all treated and non-treated septic groups compared to the sham-operated group.

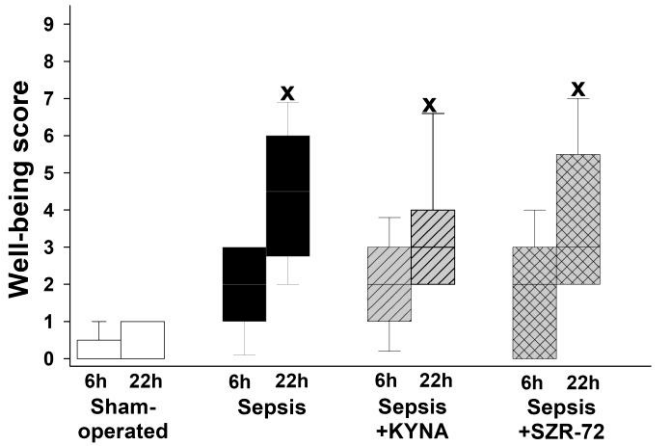

Figure 17. Changes in well-being scores 6 and 22 h after sepsis induction in the different sepsis groups treated with the saline vehicle (black box), KYNA (gray diamond/striped gray box) and SZR-72 (dark gray diamond with cross/checked gray box). The plots demonstrate the median values (horizontal line in box plots) and the 25th (lower whisker) and 75th (upper whisker) percentiles. $^{x}P<0.05$ vs. sham-operated; $^{\#}P<0.05$ vs. vehicle-treated sepsis.

4.11 Hemodynamics and oxygen dynamics

Sepsis resulted in significant hypotension during the observation period, which was not altered by the treatments (Figure 18A). HR increased significantly in two time points (the 0th and 30th min of the monitoring period) in the SZR-72 treated group (Figure 18B). As compared to sham-operated animals, a decreased PaO_2/FiO_2 ratio was observed in the vehicle-treated sepsis group, while no significant changes were found in the other groups (Figure 18C). Sepsis reduced ExO_2 values as compared to the sham-operated group, whereas both KYNA and SZR-72 resulted in a significant improvement in this parameter (Figure 18D).

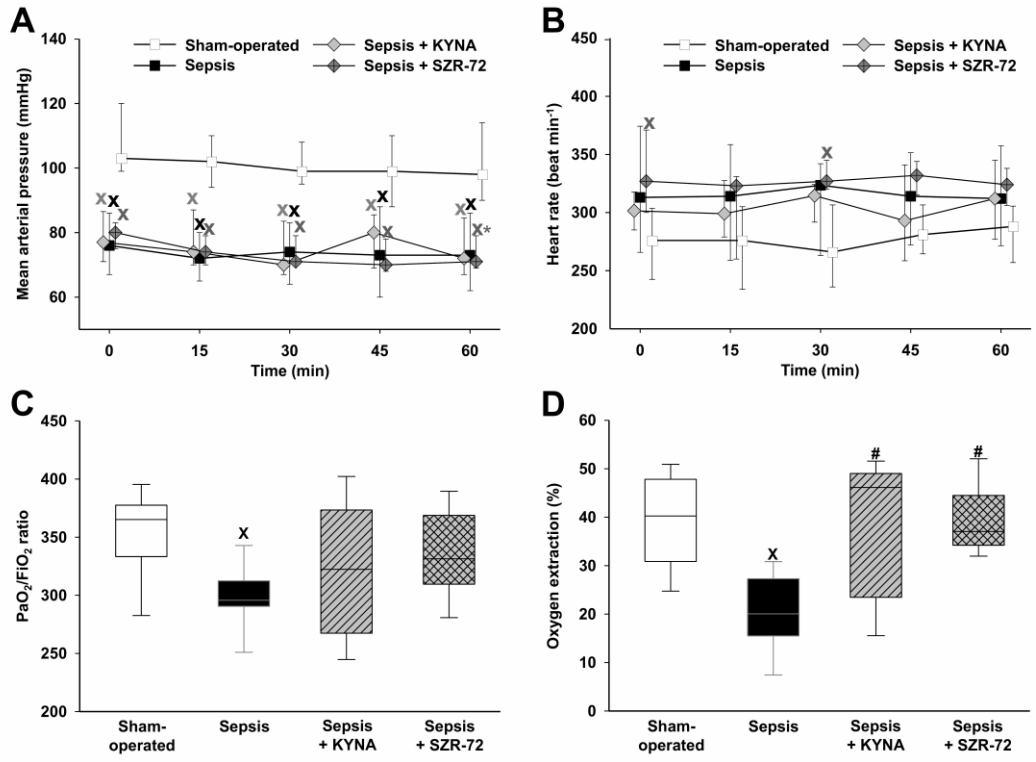

Figure 18. Time-dependent changes in mean arterial pressure (A), heart rate (B), PaO_2/FiO_2 ratio (C) and oxygen extraction (D) in the sham-operated group (empty box) and in the different sepsis groups treated with the saline vehicle (black box), KYNA (gray diamond/striped gray box) and SZR-72 (dark gray diamond with cross/checked gray box). The plots demonstrate the median values (horizontal line in box plots) and the 25th (lower whisker) and 75th (upper whisker) percentiles. $^{x}P<0.05$ vs. sham-operated; $^{\#}P<0.05$ vs. vehicle-treated sepsis; $^{*}P<0.05$ vs. 0-min.

4.12 Changes in metabolic and organ dysfunction markers

In the vehicle-treated sepsis group, plasma urea levels increased significantly, but urea levels in both treated groups were similar to those seen in the sham-operated animals (Figure 19A). Hepatic cellular damage as indicated by the De Ritis ratio was evident in the vehicle-treated and SZR-72-treated sepsis groups, whereas it did not differ between the sham-operated and KYNA-treated animals (Figure 19B). Compared to the sham-operated group, all of the groups challenged with sepsis showed a similar extent of elevation in blood lactate levels (Figure 19C). The ROFA score was significantly higher in the vehicle-treated and SZR-72-treated sepsis groups than in the sham-operated group. The ROFA values in the KYNA-treated group were not significantly different from those in the septic group (Figure 19D).

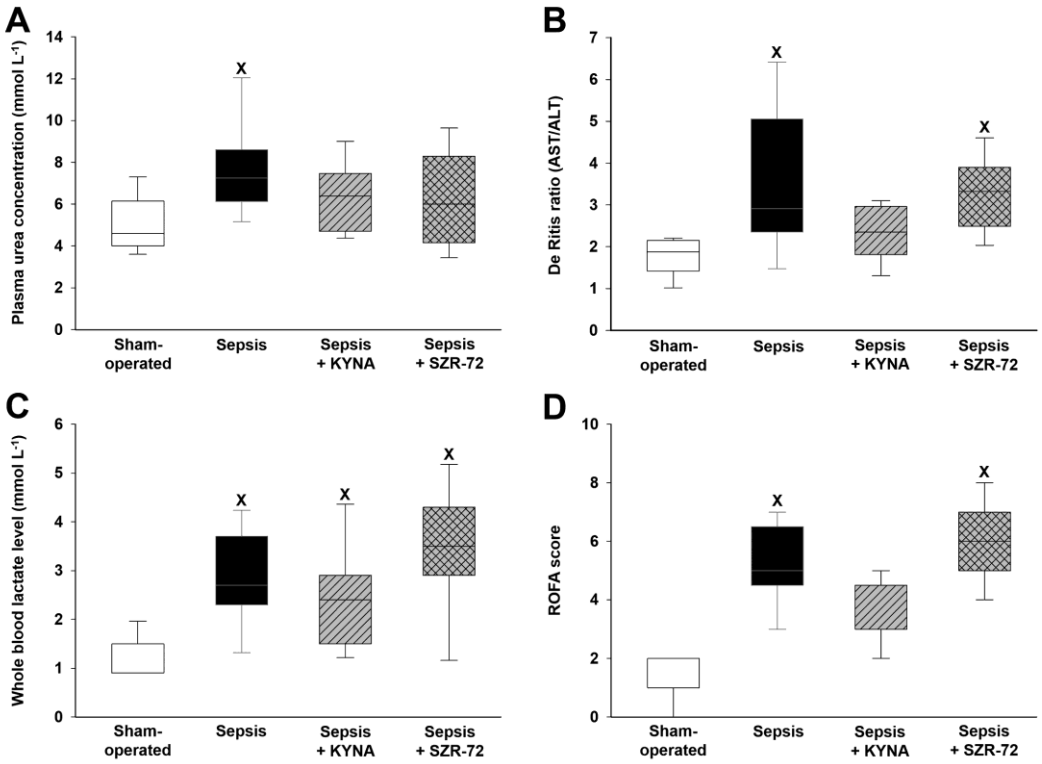

Figure 19. Changes in plasma urea (A), De Ritis ratio (AST/ALT) (B), whole blood lactate levels (C) and ROFA score values (D) in the sham-operated group (empty box) and in the different sepsis groups treated with the saline vehicle (black box), KYNA (striped gray box) and SZR-72 (checked gray box). The plots demonstrate the median (horizontal line in the box) and the 25th (lower whisker) and 75th (upper whisker) percentiles. Between groups: Kruskal–Wallis test and Dunn's post-hoc test. $^{x}P<0.05$ vs. sham-operated.

4.13 Changes in inflammatory and oxidative/nitrosative stress markers

Sepsis led to significant elevations in ET-1, IL-6, nitrotyrosine levels and XOR activity (Figure 20). All of these parameters remained, however, at the levels seen in the sham group in both the sepsis+KYNA and sepsis+SZR-72 groups.

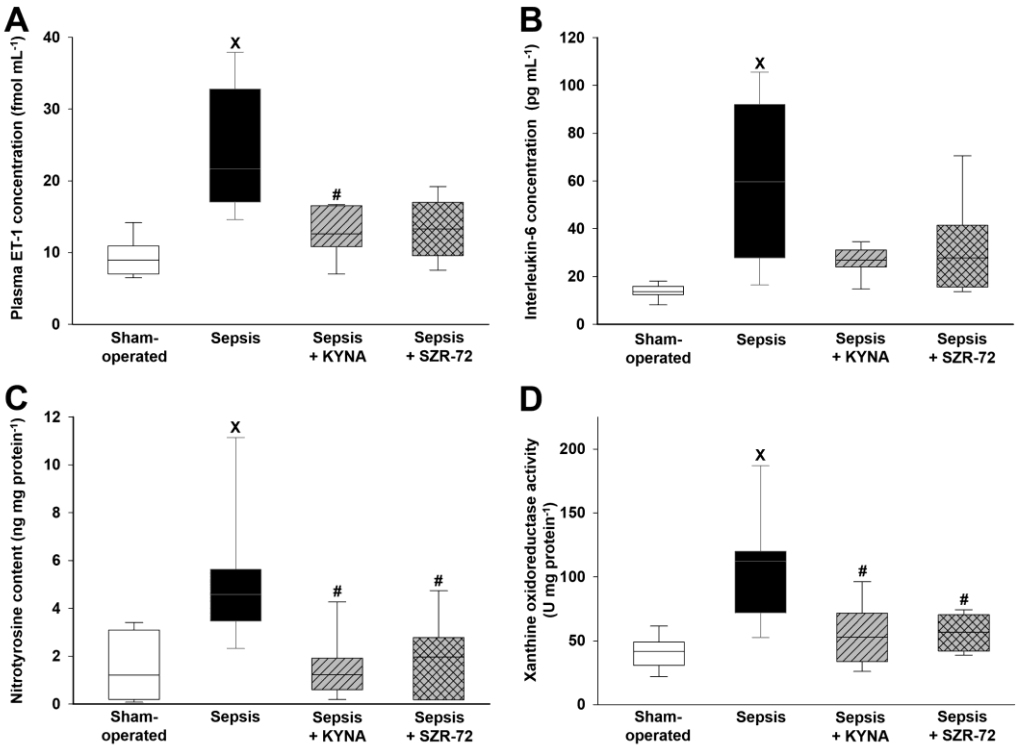

Figure 20. Changes in plasma endothelin-1 (ET-1) (A), interleukin-6 (IL-6) (B), ileal nitrotyrosine levels (C) and xanthine oxidoreductase (XOR) activity (D) in the sham-operated group (empty box) and in the different sepsis groups treated with saline (black box), KYNA (striped gray box) and SZR-72 (checked gray box). The plots demonstrate the median (horizontal line in the box) and the 25th (lower whisker) and 75th (upper whisker) percentiles. Between groups: Kruskal–Wallis test and Dunn's post-hoc test. $^{x}P<0.05$ vs. sham-operated; $^{\#}P<0.05$ vs. vehicle-treated sepsis.

4.14 Changes in mitochondrial respiration

Baseline respiration without external substrate (BLresp) and respiration following the oxidation of complex I- and complex II-linked substrates ($LEAK_{GM}$ and $LEAK_S$) were significantly decreased in sepsis (Figure 21A–B). KYNA administration did not modify sepsis-induced changes in BLresp, $LEAK_{GM}$ and $LEAK_S$. In this respect, treatment with SZR-72 preserved mitochondrial respiration with and without NADH- and $FADH_2$-linked substrates (Figure 21A–B). In addition, sepsis significantly decreased complex I- and II-linked OXPHOS. Both KYNA and SZR-72 increased complex II-linked OXPHOS capacity, while SZR-72 was able to restore complex I-linked OXPHOS completely (Figure 21A). As a result of septic insult, CI-RCR and CII-RCR were markedly decreased. These parameters

were significantly improved by KYNA and completely reversed by SZR-72 treatment (Figure 21A–B).

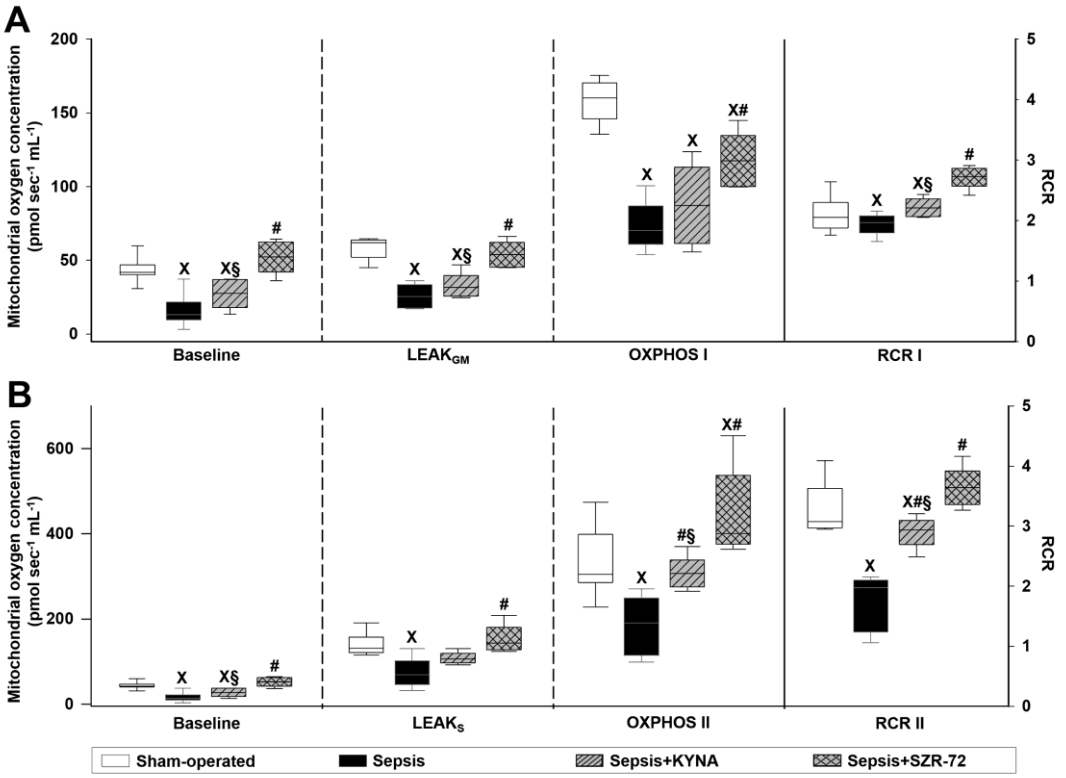

Figure 21. Baseline respiration, substrate oxidation ($LEAK_{GM}$ and $LEAK_S$), complex I- (A) and complex II-linked (B) OXPHOS capacities (OXPHOS I and OXPHOS II; left axis) and respiratory acceptor control ratios (CI, CII RCR; right axis), in the sham-operated group (empty box) and in the different sepsis groups treated with the saline vehicle (black box), KYNA (striped gray box) and SZR-72 (checked gray box). The plots illustrate the median (horizontal line in the box) and the 25th (lower whisker) and 75th (upper whisker) percentiles. $^{x}P<0.05$ vs. sham-operated; $^{\#}P<0.05$ vs. vehicle-treated sepsis; $^{\S}P<0.05$ sepsis+KYNA vs. sepsis+SZR-72.

4.15 Microcirculatory changes

Sepsis-induced microcirculatory perfusion disorders manifested in lower levels of capillary perfusion and increased perfusion heterogeneity as compared to those in the sham group (Figure 22). The values of these parameters did not differ between the sepsis and sepsis+SZR-72 groups and between the sham and sepsis+KYNA groups. KYNA was significantly more effective in ameliorating sepsis-related changes than SZR-72.

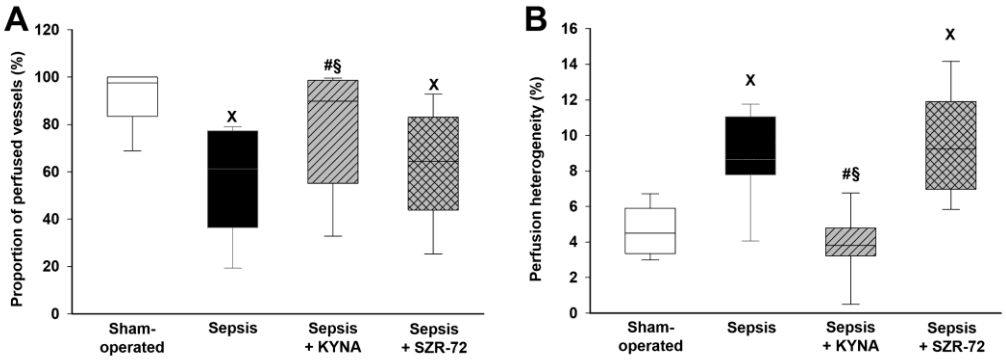

Figure 22. Changes in the proportion of perfused vessels (A) and in perfusion heterogeneity values (B) in the serosal layer of the ileum in the sham-operated group (empty box) and in the different sepsis groups treated with saline (black box), KYNA (striped gray box) and SZR-72 (checked gray box). The plots demonstrate the median (horizontal line in the box) and the 25th (lower whisker) and 75th (upper whisker) percentiles. Between groups: Kruskal–Wallis test and Dunn's post-hoc test. $^{x}P<0.05$ vs. sham-operated; $^{\#}P<0.05$ vs. vehicle-treated sepsis; $^{\S}P<0.05$ sepsis+KYNA vs. sepsis+SZR-72.

5. DISCUSSION

5.1 Overview of sepsis pathophysiology – evaluation of the model and clinical relevance

In our in vivo experimental studies, analgesia, proper fluid resuscitation, control of temperature and humane endpoints were employed according to the Minimum Quality Threshold in Pre-clinical Sepsis Studies (MQTiPSS) guidelines (Osuchowski et al. 2018). In Study 1, the inflammatory immune response was manifested in distinctive, time-dependent increases in plasma ET-1 levels in parallel with the decreasing ExO_2. These changes were most pronounced at 24 h after the induction of sepsis, suggesting that the septic reaction in rats is most severe at this time point. Additionally, similar changes were observed at 24 h of sepsis in oxygen dynamics and ET-1 release in Studies 2 and 3 as well. Here it should also be noted that 24 h in rat life corresponds to a time interval of approx. 21 days in humans, due to the often overlooked 1:21 conversion ratio of the rat-human age correlation (Sengupta et al. 2013). The changes in signs and symptoms were followed further up to 72 h, and visible and measurable parameters were monitored and recorded sequentially, again consistent with clinical practice. This approach demonstrated the resolution phase; between 24 and 72 h, the compensatory mechanisms led to recovery in the surviving cohort of animals. Therefore, a test of any treatments should be done at 24 h after induction in this model. According to the results of Study 1, the clinical relevance of the 24 h model was confirmed in Studies 2 and 3 by several changes, such as increased serum lactate level and pro-inflammatory activity together with various levels of organ dysfunction in the case of the liver, kidneys, lungs and cardiovascular system, similar to human sepsis.

Evaluation of sepsis-induced organ failure

Sepsis-induced organ injuries were characterized by our newly developed, strictly defined ROFA scoring systems based on threshold values adopted from the relevant literature (Zhai et al. 2018). The numerical parameters of cardiovascular, pulmonary, kidney and liver functions – all included in the human SOFA scoring system – established the onset of the septic reaction. Cardiovascular and respiratory dysfunctions were determined by MAP and PaO_2/FiO_2 values, respectively. In MAP scoring, anesthesia-related effects were also taken into account, whereas PaO_2/FiO_2 was used in accordance with clinical practice. Renal damage was characterized by plasma urea changes (Wang et al. 2018) based on suggested threshold values (Zhai et al. 2018). The ROFA score was supplemented with consideration

for lactate values, which is a sign of subcellular metabolic dysfunction indicative of cellular hypoxia (Zhai et al. 2018).

Role of microcirculation in sepsis

Deteriorating tissue perfusion is a key element in sepsis pathophysiology and in the development of MOF (Balestra et al. 2009). Restoration of tissue perfusion and subcellular oxygen utilization are fundamental goals in sepsis therapy (Balestra et al. 2009; Trzeciak et al. 2014). As concerns macrohemodynamics, good clinical results and improved perfusion can be achieved by supporting the cardiac pump function and volume resuscitation and promoting vasoconstriction with vasopressors (Armstrong et al. 2017). However, the price of vasopressor therapies and improved systemic hemodynamics is local vasoconstriction with depressed tissue microcirculation (Balestra et al. 2009; De Backer et al. 2014). There have been several trials of vasodilator therapies with contradictory results (Boerma et al. 2010; Trzeciak et al 2014), and it has been suggested that these fiascos may stem from an indiscriminate application of vasoactive compounds without consideration for the phase of sepsis and the degree of microcirculatory dysfunction (Inscho et al. 2005). If the microcirculation is maintained or normalized, then vasodilator therapies would no longer offer any benefit. Likewise, in the case of definite, established organ dysfunction, the use of vasodilator therapies may be futile.

Importance of mitochondria in sepsis

The decisive role of mitochondrial dysfunction leading to oxygen utilization disorders has been demonstrated in various models of endotoxemia (Doerrier et al. 2015) and sepsis (Arulkumaran et al. 2016; Crouser et al. 2004). In these studies, a considerable decrease in substrate- and ADP-stimulated respirations was accompanied by a decrease in RCR after sepsis insult. The over 10% increase in mitochondrial respiratory oxygen flux after exogenous cyt c administration following OXPHOS stimulation demonstrated that the outer mitochondrial membrane was injured in the septic animals (Bar-Or et al. 2018). This change in membrane integrity may contribute to reduced ADP-ATP conversion coupled to the electron transport system resulting in decreased RCR values. Due to the fact that a marked elevation in lactate was present, it may well be that a metabolic switch from mitochondrial oxidative phosphorylation to glycolysis (the Warburg effect) was present (Bkaily et al. 2008). Although an O_2-independent glycolytic pathway for ATP production has been documented, this alternate route may not be effective for energy production in sepsis. Of

note, ATP depletion is not a unique component of sepsis-induced mitochondrial dysfunction; organellar ROS production, elevated mitochondrial DNA level, transition pore opening-mediated apoptosis and necrosis are fundamental mitochondrial events, which lead to cellular injury (Bantel et al. 2009; Harrington et al. 2017). In addition, the release of mitochondrial components of damage-associated molecular patterns to the extracellular space may further aggravate an inflammatory response (Nakahira et al. 2015). Taken together, all these processes are intimately involved in the progression of sepsis and contribute to MOF.

5.2 Endothelin receptor-targeted therapies in sepsis

5.2.1 Circulatory effects of treatments

Effects of endothelin-A receptor antagonist treatment

We examined the ET_A-R antagonist therapy on the macro- and microhemodynamics and the main components of the cellular energy-providing mechanism. In this condition, the ET_A-R antagonist ETR-p1/fl peptide effectively improved oxygen dynamics and the splanchnic microcirculation, and displayed a tendency toward amelioration of ROFA score values. In line with these changes, we observed a non-significant elevation in the stroke volume index as well (a heart rate-independent increase in blood flow; data not shown). Selective blockage of ET_A-R has an anti-inflammatory effect (Boros et al. 1998; Szalay et al. 1998), and previous studies have already shown potentially beneficial vasodilator effects of ET_A-R antagonism in circulatory shock and sepsis (Gulati et al. 2016).

Effects of endothelin-B receptor agonist treatment

In the next step in the research procedure, the modulation of the sepsis-activated ET system was tested with ET_B-R agonist IRL-1620. This compound induced a systemic pressure response in the hypotensive septic animals with increased total peripheral resistance and improved oxygen dynamics. The intestinal capillary perfusion was also improved in this case. The beneficial effects of ET_B-R agonism have already been demonstrated in acute and chronic CNS disorders (Gulati et al. 2016; Matsuura et al. 1996) and in the peripheral circulation as well, possibly linking these reactions to vasodilator effects (Honoré et al. 2005; McMurdo et al. 1994). More importantly, it has been shown that administration of IRL-1620 also leads to tissue-dependent vasodilation or vasoconstriction; it may cause a transient decline in MAP, followed by a long-lasting pressure effect (Baranyi et al. 1998;

McMurdo et al. 1994). There are two functional subtypes of ET_B-Rs: ET_{B1}-Rs are expressed by the vascular endothelium and mediate nitric oxide-dependent vasodilatation, while ET_{B2}-Rs have a long-lasting vasopressor effect possibly due to dominant ET_A-R activity (Baranyi et al. 1998; Gulati et al. 2018; Honoré et al. 2005; McMurdo et al. 1994). It should be noted that only ET_{B1}-R is IRL-1620-sensitive, while ET_{B2}-R is IRL-1620-insensitive (Brooks et al. 1995). In our study, IRL-1620 improved the ileal capillary perfusion rate due to its local vasodilator effect or possibly through the increased microcirculatory driving pressure gradient as well.

Effects of combined endothelin-A receptor antagonist and endothelin-B receptor agonist therapy

This was the first study to investigate the microcirculatory and mitochondrial consequences of a combined ET_A-R antagonist–ET_{B1}-R agonist treatment regimen in experimental sepsis. Combining the treatments resulted in an additive effect as compared to ETR-p1/fl and IRL-1620 treatment along the global oxygen supply–demand imbalance, and the microcirculatory parameters improved further. As a final result, organ dysfunction was significantly attenuated. Our combined ET_A-R antagonist and ET_{B1}-R agonist treatment design has targeted this goal. The ET_B-Rs are heterogeneously distributed in the lungs, brain and kidneys with specific dual vasoactive effects, which can contribute to the fine tuning of tissue perfusion through either local endothelial vasodilation or vasoconstriction (Callahan et al. 2005; Davenport et al. 2016; Gulati et al. 2018). Our results suggest that if microcirculatory failure occurs, the specific inactivation of vasoconstrictor ET_A-Rs can amplify the vasomodulator effects of circulating ET-1 through the ET_B-Rs, leading to a potentially beneficial outcome at the subcellular level. Moreover, we assume that reduced ET-1 levels caused by the combined treatment may play a significant role in these processes via two potential mechanisms: first, ETR-P1/fl is an intramolecular complementary peptide of ET_A-R and can specifically bind and block ET-1 in the circulation (Corrêa et al. 2007). Second, activation of ET_{B1}-R stimulates the reuptake of circulating ET-1 (Baranyi et al. 1998; Davenport et al. 2016).

5.2.2 Mitochondrial effects of endothelin receptor-targeted therapies

In this scenario, the sepsis-associated decrease in substrate oxidation and OXPHOS was ameliorated by ET_A-R antagonist treatment. Moreover, the coupling between respiration

and phosphorylation was improved, and the functional damage to the outer membrane was also mitigated. The precise molecular mechanism by which ETR-P1/fl exerted its mitochondrial effects is not known, but the regulation of Ca^{2+} homeostasis is a plausible mechanism. It should be added that the overall interaction between the ET system and mitochondria is yet to be elucidated. The ET receptors were thought to be typical G-protein-coupled plasma membrane receptors with an intracellular signaling cascade, but Bkaily et al. recently demonstrated ET_B-Rs in the nuclear membrane, suggesting more complicated intracellular mechanisms than was previously presumed (Elustondo et al. 2015). The activation of intracellular ET_B-Rs can lead to an opening of R-type calcium channels and Na^+/Ca^{2+} exchangers (NCX), which can separately raise the intranuclear and cytoplasmatic Ca^{2+} levels and establish a complex intracellular Ca^{2+} homeostasis. If ET-1 has such extensive intracellular effects on ion fluxes, mitochondria might be part of this mechanism. Accumulation of Ca^{2+} exceeding a critical threshold (~50 μM) may lead to OXPHOS failure, an opening of the mitochondrial permeability transition pore and a depolarization of the inner mitochondrial membrane, which can ultimately lead to cell death (Goto et al. 1989). ET-1 was found to increase both the cytosolic Ca^{2+} transient (De Giusti et al. 2008) and mitochondrial ROS production (Yuki et al. 2001) and to enhance the consumption of ATP (Mino et al. 1992). It has been demonstrated that inhibition of ET_A-Rs markedly decreased mitochondrial Ca^{2+} deposition (Brunner et al. 2002) and attenuated abnormalities in Ca^{2+} sequestration (Boveris et al. 2007).

Interestingly, IRL-1620 alone did not significantly affect the key indices of mitochondrial respiratory function (a slight, statistically non-significant amelioration of CI- and CII-linked OXPHOS was detected), but supplementation with the ET_A-R antagonist resulted in a marked improvement in ADP-stimulated respiration. The question arises whether this effect is due solely to the modulation of ET_A-Rs or both ET_A-Rs and ET_{B1}-Rs. Despite the fact that IRL-1620 itself was not effective, an indirect action through the improvement of O_2 delivery/extraction cannot be ruled out. A more effective O_2 extraction in the tissues provides better O_2 diffusion to mitochondria, where it can be reduced by the ETS to support ATP synthesis (Tykocki et al. 2010). However, it remains unclear whether the recovery of mitochondrial function mediated by the modulation of ET receptors (Singer et al. 2016) is a consequence of an improved microcirculatory dysfunction (Armstrong et al. 2017), a direct action on the organelle or (Balestra et al. 2009) a result of both mechanisms at the same time. The direct mitochondrial effect of ET-1 on elevated mitochondrial ROS

production has previously been reported (Yuki et al. 2001). Nevertheless, the presence of ET receptors has only been confirmed in the nucleus to date. If the receptor were located on other organelles, e.g. the mitochondria or endoplasmic reticulum, this would influence various signaling processes, such as calcium transport, respiration or apoptosis (Moullan et al. 2015).

5.3 Divergent effects of kynurenic acid and SZR-72

Effects of kynurenic acid and SZR-72 on septic organ failure

Study 3 demonstrates the distinct effects of KYNA and its synthetic analogue on microcirculation and mitochondrial function in experimental sepsis. A novel, rat-specific scoring system was used to trace the development of MOF in this rat sepsis model and to indicate differences between the efficacy of KYNA and SZR-72. Both treatments reduced lung and kidney dysfunctions to a similar extent due to the decreased level of inflammatory markers and their enhanced antioxidant/anti-nitrosative effect. However, only the KYNA treatment reduced hypoxia-sensitive ET-1 levels and displayed a tendency toward amelioration of liver injury and ROFA score values.

Effects of kynurenic acid and SZR-72 on ileal microperfusion

We have observed that both KYNA and SZR-72 prevented a sepsis-induced decrease in oxygen extraction to the same extent, but only KYNA ameliorated sepsis-related microcirculatory perfusion deficit (reduction in capillary perfusion and an increase in perfusion heterogeneity) significantly. This distinct effect of compounds is possibly due to their different structure- and receptor-related characteristics (Mándi et al. 2019). The potential direct microcirculatory effects of KYNA in the ileum are unknown, but it has been shown to increase global and cortical renal blood flow (and to improve renal excretion) under physiological conditions and to reduce renal oxidative stress during ischemia–reperfusion injury (Badzynska et al. 2014; Pundir et al. 2013). Based on our results, some of these micro-hemodynamic effects can also be linked to a reduced ET-1 release elicited by KYNA. NMDA receptor-related microcirculation improvement can be explained by many mechanisms. Firstly, antagonism of NMDA receptors expressed on the surface of smooth muscle cells brings about reduced intracellular Ca2+ levels (Wirthgen et al. 2017), resulting in smooth muscle relaxation (Adelstein et al. 1987). On the other hand, a reduction of the levels of pro-inflammatory IL-6, XOR activity and ROS sensitive vasoconstrictor

ET-1 release by KYNA may attenuate the cytokine- and ROS-induced vasoconstriction of microvessels. Although the use of vasodilator therapy in sepsis is debated (Boerma et al. 2010; Moore et al. 2015; Trzeciak et al. 2014), a reduction of circulating ET-1 levels through a combined ET receptor-targeted treatment regimen has been demonstrated to ameliorate microcirculatory deficit in sepsis (Study 2). Further, KYNA may also act as an agonist for the orphan receptor GPR35 and reduce inflammation independently of the NMDA receptors. This receptor is expressed at high levels in intestine and immune cells (Wang et al. 2006), and the concentrations of KYNA required to induce effects differ between NMDA-R and GPR35. Compared with NMDA-R, lower concentrations of KYNA are able to elicit a response when binding to GPR35 (Turski et al. 2013). Taking into account that (1) KYNA is an endogenous ligand for GPR35 and that (2) only KYNA, but not the synthetic analogue, was able to restore the perfusion disturbances in the ileum, a GPR35-mediated mechanism cannot be ruled out.

Effects of kynurenic acid and SZR-72 on mitochondrial respiration

KYNA- and its analogue-based treatments also had different effects on mitochondrial function, with the ameliorating effects of SZR-72 being more pronounced. The role of endogenous KYNA on mitochondrial physiology is still unmapped; however, exogenous KYNA was able to improve OXPHOS II without affecting OXPHOS I. This difference in complex activities may arise from the fact that complex I is more susceptible to cellular injury than complex II. Oxidation of glutamate requires pyridine nucleotides, and these in conjunction with other cofactors may be lost during sepsis (Hart et al. 2003). Our findings are consistent with a study by Ferreira et al. (2018), in which KYNA ameliorated several aspects of mitochondrial function in a neurodegeneration model. Similar to our results, KYNA administration significantly improved succinate dehydrogenase activity. In addition, KYNA preserved mitochondrial mass, enhanced antioxidant enzyme levels, and reduced ROS production after quinolinic acid-induced cell injury (Ferreira et al. 2018). In adipose tissue, KYNA modulated energy utilization (increased lipid metabolism and mitochondrial respiration) via a GPR35 pathway (Agudelo et al. 2018). In our experiments, administration of SZR-72 markedly improved the key indices of mitochondrial function.

Previous studies with the KYNA analogue revealed a more pronounced anti-inflammatory response in animal models of colitis and neuroinflammation than that seen with KYNA (Kaszaki et al. 2012; Knyihar-Csillik et al. 2008; Lukács et al. 2017), but both KYNA and

SZR-72 reduced oxidative/nitrosative stress marker levels [XOR, nitric oxide synthase (NOS) and myeloperoxidase (MPO) activities] (Kaszaki et al. 2012) and attenuated glutamate expression (Lukács et al. 2017). KYNA inhibits the release of glutamate (Carpenedo et al., 2001), TNFα (Wang et al. 2006) and α7 nicotinic receptor activity (Hilmas et al. 2001), amplifies the effect of endogenous opioid receptor agonists (e.g. endomorphin-1; Mecs et al. 2009) and stimulates the Nrf2-antioxidant response pathway (Ferreira et al. 2018).

Compared to KYNA, the effects of SZR-72 were more pronounced in this sepsis model, and a remarkable increase in ADP-stimulated respirations (OXPHOS I and II) and RCR were found in liver homogenate after sepsis induction. Preservation of these parameters is fundamental for better O_2 utilization (less ETS-linked ROS is generated) and maintenance of ATP production (Zorova et al. 2018). Although the ETS-independent pathway for ATP production is well documented in the literature (glycolytic ATP production) and it may well be that it is present in sepsis (elevated blood lactate), this alternate route is not efficient for energy production (2 ATP versus 36 ATP molecules per glucose; Yetkin-Arik et al. 2019). Several hypotheses may explain the mechanism behind the more advantageous mitochondrial effects of SZR-72. First, the physico-chemical properties of KYNA and SZR-72 are different, thus possibly influencing crossing through the BBB and membranes (Knyihar-Csillik;et al 2008). There is evidence that KYNA only crosses the BBB poorly, whereas SZR-72 is BBB-permeable due to a water-soluble side chain with an extra cationic center (Fülöp et al. 2012; Vécsei et al. 2013). Apart from BBB, a facilitated membrane crossing of SZR-72 may affect intracellular signaling, including the activation of antioxidative/anti-apoptotic pathways. A second scenario is a distinct molecule binding at the NMDA-R glycine site. More recently, NMDA-Rs were shown to be present in the inner mitochondrial membrane (mtNMDA-R) (Nesterov et al. 2018), where they may play a regulative role in (1) Ca2+ transport, (2) ROS production and (3) metabolic switching during hypoxia (Selin et al. 2016). Under these circumstances, it may well be that SZR-72 has a much higher affinity for either plasma membrane or mtNMDAR than KYNA. In addition, a protein–protein interaction between NMDA-R and an ND2 subunit of complex I was found through an Src adapter protein (Gingrich et al. 2004). It cannot be ruled out that KYNA and SZR-72 influence this interaction and regulate mitochondrial homeostasis differently. The influence of sepsis on NMDA-R expression and glutamate levels is incompletely characterized. We did not examine changes in NMDA-R subunits due to

technical limitations, but other laboratories have found a marked increase in lung NR1 and NR2A contents in a cecal ligation and puncture (CLP) sepsis model. Furthermore, treatment with the NMDA-R antagonist MK-801 lowered lactate dehydrogenase and oxidative damage and improved survival 144 h after sepsis induction in rats (da Cunha et al. 2010). Similarly, survival was markedly increased (by 80%), and markers of inflammation were reduced in MK-801-treated mice 48 h after lipopolysaccharide (LPS) stimuli (Zhe et al. 2018). In this model, LPS also raised the glutamate level in bronchoalveolar lavage fluid. Based on these findings and the fact that KYNA is a natural antagonist, a similar, NMDA-R-linked mechanism, at least in part, cannot be ruled out in our polymicrobial sepsis model.

5.4 Limitations

It is important to note that these studies have some limitations. First, the observation timeline was relatively short in Studies 2 and 3, and therefore longer endpoints, such as mortality, with longer pharmacological effects should also be examined in follow-up studies. Our newly described ROFA score also seems to be a potentially useful tool for this purpose, but it will be necessary to validate the system under other experimental conditions as well. Second, the effect of the ketamine-containing anesthesia on the results cannot be disregarded. Third, it is important to note that, despite our intention to follow all of the recommendations in the MQTiPSS guidelines, antimicrobial therapy was excluded from the protocols for a few reasons, most importantly because of the known influence of antibiotics on mitochondrial respiration (Moullan et al. 2015; Piechota-Polanczyk et al. 2018), which was the focus of the thesis. Moreover, the relatively short protocol and monitoring did not provide sufficient time to evaluate the effectiveness of antibiotic therapy. Controlling the efficacy of antibiotic therapy by detecting the plasma procalcitonin level or using the result of blood culture would require a longer experimental protocol (Trásy et al. 2016). This suggests that the ineffectiveness of empirically applied antibiotic therapy (30% of clinical cases) could greatly influence the results (Mettler et al. 2007).

6. SUMMARY OF NEW FINDINGS

1. We designed and described a clinically relevant rat model of intraabdominal sepsis, characterized by organ dysfunctions, together with complex macro/microcirculatory and mitochondrial dysfunction.

2. We demonstrated that ET receptors could indirectly influence mitochondrial function through the mechanism of tissue perfusion and restoration of the intracellular oxygen supply. The selective ET_B-R agonist countervailed the peritonitis-induced hypotension, while the ET_A-R antagonist maintained microcirculation and oxygen dynamics. A mixed ET receptor-targeted treatment regime may offer a novel possibility for a simultaneous microcirculatory and mitochondrial resuscitation strategy by also reducing circulating ET-1 levels and ameliorating inflammatory indices of sepsis.

3. Treatments with KYNA and its synthetic analogue attenuated the deleterious consequences of oxidative/nitrosative stress and resulted in lower inflammatory mediator release. Administration of SZR-72 may directly regulate mitochondrial respiration and ATP synthesis, whereas treatment with KYNA primarily ameliorates microcirculatory dysfunction and therefore restores organelle function.

4. Despite compartmentalization, microcirculatory and mitochondrial functions are closely linked under physiological circumstances. The common denominator in both mechanisms may be the capillary-mitochondrial oxygen gradient, which may be a decisive factor in mitochondrial function in sepsis. Therefore, the efficacy of microcirculatory resuscitation therapies should be apparent at the subcellular level as well.

7. ACKNOWLEDGEMENTS

I would like to express my gratitude to Professor Mihály Boros, head of the Institute of Surgical Research, for his immense knowledge and valuable scientific guidance. I greatly appreciate his encouragement and thank him for providing me the opportunity to carry out my research and for initiating my scientific career in the institute.

I am especially grateful to my supervisor and mentor, József Kaszaki, for his personal guidance and continuous support in helping me acquire experimental skills. Without his ongoing support, interest and stimulating guidance, my doctoral thesis could hardly have come to fruition.

I am grateful to the co-workers in our research group, László Juhász, Szabolcs Péter Tallósy, Marietta Zita Poles, Anna Nászai, Roland Fejes and Andrea Szabó, for their help and valuable work in improving the scientific value of the studies in this PhD thesis.

I would like to thank my colleagues Dániel Érces and Gabriella Varga for their help in acquiring experimental surgical skills and for the great trust with which they involved me in their research.

I wish to express my thanks for the excellent technical assistance at the Institute of Surgical Research and for the help I received from Csilla Mester, Annamária Kócsó, Nikolett Beretka Zádori, Andrea Bús, Virág Molnár, Éva Nagyiván, Bence Győrfi and István Szabó.

And last, but not least, I wish to thank my mother, grandfather, brother and indeed all my family and friends for their never-ending love, support and patience. Without them, I could never achieve my goals.

Sources of funding: NKFIH K116689, GINOP-2.3.2-15-2016-00034;

Supported by the ÚNKP-20-4 - New National Excellence Program of the Ministry for Innovation and Technology from the Source of the National Research, Development and Innovation Fund.

8. REFERENCES

1. Adelstein RS, Sellers JR. Effects of calcium on vascular smooth muscle contraction. Am J Cardiol. 1987 Jan 30;59(3):4B-10B. doi: 10.1016/0002-9149(87)90076-2. PMID: 3028118.

2. Agudelo LZ, Ferreira DMS, Cervenka I, Bryzgalova G, Dadvar S, Jannig PR, Pettersson-Klein AT, Lakshmikanth T, Sustarsic EG, Porsmyr-Palmertz M, Correia JC, Izadi M, Martínez-Redondo V, Ueland PM, Midttun Ø, Gerhart-Hines Z, Brodin P, Pereira T, Berggren PO, Ruas JL. Kynurenic Acid and Gpr35 Regulate Adipose Tissue Energy Homeostasis and Inflammation. Cell Metab. 2018 Feb 6;27(2):378-392.e5. doi: 10.1016/j.cmet.2018.01.004. PMID: 29414686

3. Armstrong BA, Betzold RD, May AK. Sepsis and Septic Shock Strategies. Surg Clin North Am. 2017 Dec;97(6):1339-1379. doi: 10.1016/j.suc.2017.07.003. Epub 2017 Oct 5. PMID: 29132513.

4. Arulkumaran N, Deutschman CS, Pinsky MR, Zuckerbraun B, Schumacker PT, Gomez H, Gomez A, Murray P, Kellum JA; ADQI XIV Workgroup. MITOCHONDRIAL FUNCTION IN SEPSIS. Shock. 2016 Mar;45(3):271-81. doi: 10.1097/SHK.0000000000000463. PMID: 26871665; PMCID: PMC4755359.

5. Aykut G, Veenstra G, Scorcella C, Ince C, Boerma C. Cytocam-IDF (incident dark field illumination) imaging for bedside monitoring of the microcirculation. Intensive Care Med Exp. 2015 Dec;3(1):40. doi: 10.1186/s40635-015-0040-7. Epub 2015 Jan 31. PMID: 26215807; PMCID: PMC4512989.

6. Bądzyńska B, Zakrocka I, Sadowski J, Turski WA, Kompanowska-Jezierska E. Effects of systemic administration of kynurenic acid and glycine on renal haemodynamics and excretion in normotensive and spontaneously hypertensive rats. Eur J Pharmacol. 2014 Nov 15;743:37-41. doi: 10.1016/j.ejphar.2014.09.020. Epub 2014 Sep 28. PMID: 25263305.

7. Balestra GM, Legrand M, Ince C. Microcirculation and mitochondria in sepsis: getting out of breath. Curr Opin Anaesthesiol. 2009 Apr;22(2):184-90. doi: 10.1097/ACO.0b013e328328d31a. PMID: 19307893.

8. Bantel H, Schulze-Osthoff K. Cell death in sepsis: a matter of how, when, and where. Crit Care. 2009;13(4):173. doi: 10.1186/cc7966. Epub 2009 Jul 31. PMID: 19678906; PMCID: PMC2750164.

9. Baranyi L, Campbell W, Ohshima K, Fujimoto S, Boros M, Okada H. The antisense homology box: a new motif within proteins that encodes biologically active peptides. Nat Med. 1995 Sep;1(9):894-901. doi: 10.1038/nm0995-894. PMID: 7585214.

10. Baranyi L, Campbell W, Ohshima K, Fujimoto S, Boros M, Kaszaki J, Okada H. Antisense homology box-derived peptides represent a new class of endothelin receptor inhibitors. Peptides. 1998;19(2):211-23. doi: 10.1016/s0196-9781(97)00370-7. PMID: 9493852.

11. Bar-Or D, Carrick M, Tanner A 2nd, Lieser MJ, Rael LT, Brody E. Overcoming the Warburg Effect: Is it the key to survival in sepsis? J Crit Care. 2018 Feb;43:197-201. doi: 10.1016/j.jcrc.2017.09.012. Epub 2017 Sep 8. PMID: 28915394.

12. Beckman JS, Parks DA, Pearson JD, Marshall PA, Freeman BA. A sensitive fluorometric assay for measuring xanthine dehydrogenase and oxidase in tissues. Free Radic Biol Med. 1989;6(6):607-15. doi: 10.1016/0891-5849(89)90068-3. PMID: 2753392.

13. Bkaily G, Choufani S, Avedanian L, Ahmarani L, Nader M, Jacques D, D'Orléans-Juste P, Al Khoury J. Nonpeptidic antagonists of ETA and ETB receptors reverse the ET-1-induced sustained increase of cytosolic and nuclear calcium in human aortic vascular smooth muscle cells. Can J Physiol Pharmacol. 2008 Aug;86(8):546-56. doi: 10.1139/Y08-048. PMID: 18758503.

14. Boerma EC, Koopmans M, Konijn A, Kaiferova K, Bakker AJ, van Roon EN, Buter H, Bruins N, Egbers PH, Gerritsen RT, Koetsier PM, Kingma WP, Kuiper MA, Ince C. Effects of nitroglycerin on sublingual microcirculatory blood flow in patients with severe sepsis/septic shock after a strict resuscitation protocol: a double-blind randomized placebo controlled trial. Crit Care Med. 2010 Jan;38(1):93-100. doi: 10.1097/CCM.0b013e3181b02fc1. PMID: 19730258.

15. Bone RC, Balk RA, Cerra FB, Dellinger RP, Fein AM, Knaus WA, Schein RM, Sibbald WJ. Definitions for sepsis and organ failure and guidelines for the use of innovative therapies in sepsis. The ACCP/SCCM Consensus Conference Committee. American College of Chest Physicians/Society of Critical Care Medicine. Chest. 1992 Jun;101(6):1644-55. doi: 10.1378/chest.101.6.1644. PMID: 1303622.

16. Boros M, Massberg S, Baranyi L, Okada H, Messmer K. Endothelin 1 induces leukocyte adhesion in submucosal venules of the rat small intestine. Gastroenterology. 1998 Jan;114(1):103-14. doi: 10.1016/s0016-5085(98)70638-9. PMID: 9428224.

17. Boveris DL, Boveris A. Oxygen delivery to the tissues and mitochondrial respiration. Front Biosci. 2007 Jan 1;12:1014-23. doi: 10.2741/2121. PMID: 17127356.

18. Brooks DP, DePalma PD, Pullen M, Gellai M, Nambi P. Identification and function of putative ETB receptor subtypes in the dog kidney. J Cardiovasc Pharmacol. 1995;26 Suppl 3:S322-5. PMID: 8587403.

19. Brunner F, Wölkart G, Haleen S. Defective intracellular calcium handling in monocrotaline-induced right ventricular hypertrophy: protective effect of long-term endothelin-A receptor blockade with 2-benzo[1,3]dioxol-5-yl-3-benzyl-4-(4-methoxy-phenyl-)- 4-oxobut-2-enoate-sodium (PD 155080). J Pharmacol Exp Ther. 2002 Feb;300(2):442-9. doi: 10.1124/jpet.300.2.442. PMID: 11805203.

20. Callahan LA, Supinski GS. Sepsis induces diaphragm electron transport chain dysfunction and protein depletion. Am J Respir Crit Care Med. 2005 Oct 1;172(7):861-8. doi: 10.1164/rccm.200410-1344OC. Epub 2005 Jun 30. PMID: 15994462.

21. Carpenedo R, Pittaluga A, Cozzi A, Attucci S, Galli A, Raiteri M, Moroni F. Presynaptic kynurenate-sensitive receptors inhibit glutamate release. Eur J Neurosci. 2001 Jun;13(11):2141-7. doi: 10.1046/j.0953-816x.2001.01592.x. PMID: 11422455.

22. Chousterman BG, Swirski FK, Weber GF. Cytokine storm and sepsis disease pathogenesis. Semin Immunopathol. 2017 Jul;39(5):517-528. doi: 10.1007/s00281-017-0639-8. Epub 2017 May 29. PMID: 28555385

23. Corrêa TD, Filho RR, Assunção MS, Silva E, Lima A. Vasodilators in Septic Shock Resuscitation: A Clinical Perspective. Shock. 2017 Mar;47(3):269-275. doi: 10.1097/SHK.0000000000000777. PMID: 27787407.

24. Crouser ED, Julian MW, Huff JE, Joshi MS, Bauer JA, Gadd ME, Wewers MD, Pfeiffer DR. Abnormal permeability of inner and outer mitochondrial membranes contributes independently to mitochondrial dysfunction in the liver during acute endotoxemia. Crit Care Med. 2004 Feb;32(2):478-88. doi: 10.1097/01.CCM.0000109449.99160.81. PMID: 14758167.

25. Dabrowski W, Kocki T, Pilat J, Parada-Turska J, Malbrain ML. Changes in plasma kynurenic acid concentration in septic shock patients undergoing continuous veno-venous haemofiltration. Inflammation. 2014 Feb;37(1):223-34. doi: 10.1007/s10753-013-9733-9. PMID: 24043287; PMCID: PMC3929023.

26. da Cunha AA, Pauli V, Saciura VC, Pires MG, Constantino LC, de Souza B, Petronilho F, Rodrigues de Oliveira J, Ritter C, Romão PR, Boeck CR, Roesler R, Quevedo J, Dal-Pizzol F. N-methyl-D-aspartate glutamate receptor blockade attenuates lung injury associated with experimental sepsis. Chest. 2010 Feb;137(2):297-302. doi: 10.1378/chest.09-1570. Epub 2009 Oct 16. PMID: 19837828.

27. Davenport AP, Hyndman KA, Dhaun N, Southan C, Kohan DE, Pollock JS, Pollock DM, Webb DJ, Maguire JJ. Endothelin. Pharmacol Rev. 2016 Apr;68(2):357-418. doi: 10.1124/pr.115.011833. PMID: 26956245; PMCID: PMC4815360.

28. De Backer D, Orbegozo Cortes D, Donadello K, Vincent JL. Pathophysiology of microcirculatory dysfunction and the pathogenesis of septic shock. Virulence. 2014 Jan 1;5(1):73-9. doi: 10.4161/viru.26482. Epub 2013 Sep 25. PMID: 24067428; PMCID: PMC3916386.

29. De Backer D, Hollenberg S, Boerma C, Goedhart P, Büchele G, Ospina-Tascon G, Dobbe I, Ince C. How to evaluate the microcirculation: report of a round table conference. Crit Care. 2007;11(5):R101. doi: 10.1186/cc6118. PMID: 17845716; PMCID: PMC2556744.

30. De Giusti VC, Correa MV, Villa-Abrille MC, Beltrano C, Yeves AM, de Cingolani GE, Cingolani HE, Aiello EA. The positive inotropic effect of endothelin-1 is mediated by mitochondrial reactive oxygen species. Life Sci. 2008 Aug 15;83(7-8):264-71. doi: 10.1016/j.lfs.2008.06.008. Epub 2008 Jun 24. PMID: 18625248.

31. Dejager L, Pinheiro I, Dejonckheere E, Libert C. Cecal ligation and puncture: the gold standard model for polymicrobial sepsis? Trends Microbiol. 2011 Apr;19(4):198-208. doi: 10.1016/j.tim.2011.01.001. PMID: 21296575.

32. Delano MJ, Ward PA. The immune system's role in sepsis progression, resolution, and long-term outcome. Immunol Rev. 2016 Nov;274(1):330-353. doi: 10.1111/imr.12499. PMID: 27782333; PMCID: PMC5111634.

33. Doerrier C, García JA, Volt H, Díaz-Casado ME, Lima-Cabello E, Ortiz F, Luna-Sánchez M, Escames G, López LC, Acuña-Castroviejo D. Identification of mitochondrial deficits and melatonin targets in liver of septic mice by high-resolution respirometry. Life Sci. 2015 Jan 15;121:158-65. doi: 10.1016/j.lfs.2014.11.031. Epub 2014 Dec 10. PMID: 25498899.

34. Doerrier C, Garcia-Souza LF, Krumschnabel G, Wohlfarter Y, Mészáros AT, Gnaiger E. High-Resolution FluoRespirometry and OXPHOS Protocols for Human Cells, Permeabilized Fibers from Small Biopsies of Muscle, and Isolated Mitochondria. Methods Mol Biol. 2018;1782:31-70. doi: 10.1007/978-1-4939-7831-1_3. PMID: 29850993.

35. Dubin A, Kanoore Edul VS, Caminos Eguillor JF, Ferrara G. Monitoring Microcirculation: Utility and Barriers - A Point-of-View Review. Vasc Health Risk Manag. 2020 Dec 31;16:577-589. doi: 10.2147/VHRM.S242635. PMID: 33408477; PMCID: PMC7780856.

36. Eichacker PQ, Parent C, Kalil A, Esposito C, Cui X, Banks SM, Gerstenberger EP, Fitz Y, Danner RL, Natanson C. Risk and the efficacy of antiinflammatory agents: retrospective and confirmatory studies of sepsis. Am J Respir Crit Care Med. 2002 Nov 1;166(9):1197-205. doi: 10.1164/rccm.200204-302OC. PMID: 12403688.

37. Elustondo PA, Negoda A, Kane CL, Kane DA, Pavlov EV. Spermine selectively inhibits high-conductance, but not low-conductance calcium-induced permeability transition pore. Biochim Biophys Acta. 2015 Feb;1847(2):231-240. doi: 10.1016/j.bbabio.2014.10.007. Epub 2014 Nov 1. PMID: 25448536.

38. Esposito S, De Simone G, Boccia G, De Caro F, Pagliano P. Sepsis and septic shock: New definitions, new diagnostic and therapeutic approaches. J Glob Antimicrob Resist. 2017 Sep;10:204-212. doi: 10.1016/j.jgar.2017.06.013. Epub 2017 Jul 22. PMID: 28743646.

39. Érces D, Zsikai B, Bizanc L, Sztanyi P, Vida G , Boros M, Jiga L, Ionac M, Mandi Y, Kaszaki J. An improved model of severe sepsis in pigs. TMJ 2011, Vol. 61, No. 3 - 4

40. Érces D, Varga G, Fazekas B, Kovács T, Tőkés T, Tiszlavicz L, Fülöp F, Vécsei L, Boros M, Kaszaki J. N-methyl-D-aspartate receptor antagonist therapy suppresses colon motility and inflammatory activation six days after the onset of experimental colitis in rats. Eur J Pharmacol. 2012 Sep 15;691(1-3):225-34. doi: 10.1016/j.ejphar.2012.06.044. Epub 2012 Jul 14. PMID: 22796676.

41. Ferreira FS, Biasibetti-Brendler H, Pierozan P, Schmitz F, Bertó CG, Prezzi CA, Manfredini V, Wyse ATS. Kynurenic Acid Restores Nrf2 Levels and Prevents Quinolinic Acid-Induced Toxicity in Rat Striatal Slices. Mol Neurobiol. 2018 Nov;55(11):8538-8549. doi: 10.1007/s12035-018-1003-2. Epub 2018 Mar 21. PMID: 29564809.

42. Forni M, Mazzola S, Ribeiro LA, Pirrone F, Zannoni A, Bernardini C, Bacci ML, Albertini M. Expression of endothelin-1 system in a pig model of endotoxic shock. Regul Pept. 2005 Nov;131(1-3):89-96. doi: 10.1016/j.regpep.2005.07.001. PMID: 16043243.

43. Fülöp F, Szatmári I, Vámos E, Zádori D, Toldi J, Vécsei L. Syntheses, transformations and pharmaceutical applications of kynurenic acid derivatives. Curr Med Chem. 2009;16(36):4828-42. doi: 10.2174/092986709789909602. PMID: 19929784.

44. Fülöp F, Szatmári I, Toldi J, Vécsei L. Modifications on the carboxylic function of kynurenic acid. J Neural Transm (Vienna). 2012 Feb;119(2):109-14. doi: 10.1007/s00702-011-0721-7. Epub 2011 Oct 14. PMID: 21997444.

45. Freeman BD, Natanson C. Anti-inflammatory therapies in sepsis and septic shock. Expert Opin Investig Drugs. 2000 Jul;9(7):1651-63. doi: 10.1517/13543784.9.7.1651. PMID: 11060768.

46. Goto K, Kasuya Y, Matsuki N, Takuwa Y, Kurihara H, Ishikawa T, Kimura S, Yanagisawa M, Masaki T. Endothelin activates the dihydropyridine-sensitive, voltage-dependent Ca2+ channel in vascular smooth muscle. Proc Natl Acad Sci U S A. 1989 May;86(10):3915-8. doi: 10.1073/pnas.86.10.3915. PMID: 2542956; PMCID: PMC287252.

47. Goto T, Hussein MH, Kato S, Daoud GA, Kato T, Kakita H, Mizuno H, Imai M, Ito T, Kato I, Suzuki S, Okada N, Togari H, Okada H. Endothelin receptor antagonist attenuates inflammatory response and prolongs the survival time in a neonatal sepsis model. Intensive Care Med. 2010 Dec;36(12):2132-9. doi: 10.1007/s00134-010-2040-0. Epub 2010 Sep 16. PMID: 20845025.

48. Gulati A. Endothelin Receptors, Mitochondria and Neurogenesis in Cerebral Ischemia. Curr Neuropharmacol. 2016;14(6):619-26. doi: 10.2174/1570159x14666160119094959. PMID: 26786146; PMCID: PMC4981738.

49. Gulati A, Hornick MG, Briyal S, Lavhale MS. A novel neuroregenerative approach using ET(B) receptor agonist, IRL-1620, to treat CNS disorders. Physiol Res. 2018 Jun 27;67(Suppl 1):S95-S113. doi: 10.33549/physiolres.933859. PMID: 29947531.

50. Gingrich JR, Pelkey KA, Fam SR, Huang Y, Petralia RS, Wenthold RJ, Salter MW. Unique domain anchoring of Src to synaptic NMDA receptors via the mitochondrial protein NADH dehydrogenase subunit 2. Proc Natl Acad Sci U S A. 2004 Apr 20;101(16):6237-42. doi: 10.1073/pnas.0401413101. Epub 2004 Apr 6. Erratum in: Proc Natl Acad Sci U S A. 2006 Jun 20;103(25):9744. PMID: 15069201; PMCID: PMC395953.

51. Harrington JS, Choi AMK, Nakahira K. Mitochondrial DNA in Sepsis. Curr Opin Crit Care. 2017 Aug;23(4):284-290. doi: 10.1097/MCC.0000000000000427. PMID: 28562385; PMCID: PMC5675027.

52. Hart DW, Gore DC, Rinehart AJ, Asimakis GK, Chinkes DL. Sepsis-induced failure of hepatic energy metabolism. J Surg Res. 2003 Nov;115(1):139-47. doi: 10.1016/s0022-4804(03)00284-1. PMID: 14572785.

53. Hilmas C, Pereira EF, Alkondon M, Rassoulpour A, Schwarcz R, Albuquerque EX. The brain metabolite kynurenic acid inhibits alpha7 nicotinic receptor activity and increases non-alpha7 nicotinic receptor expression: physiopathological implications. J Neurosci. 2001 Oct 1;21(19):7463-73. doi: 10.1523/JNEUROSCI.21-19-07463.2001. PMID: 11567036; PMCID: PMC6762893.

54. Hogan-Cann AD, Anderson CM. Physiological Roles of Non-Neuronal NMDA Receptors. Trends Pharmacol Sci. 2016 Sep;37(9):750-767. doi: 10.1016/j.tips.2016.05.012. Epub 2016 Jun 21. PMID: 27338838

55. Honoré JC, Fecteau MH, Brochu I, Labonté J, Bkaily G, D'Orleans-Juste P. Concomitant antagonism of endothelial and vascular smooth muscle cell ETB receptors for endothelin induces hypertension in the hamster. Am J Physiol Heart Circ Physiol. 2005 Sep;289(3):H1258-64. doi: 10.1152/ajpheart.00352.2005. Epub 2005 May 6. PMID: 15879484.

56. Ince C, Mik EG. Microcirculatory and mitochondrial hypoxia in sepsis, shock, and resuscitation. J Appl Physiol (1985). 2016 Jan 15;120(2):226-35. doi: 10.1152/japplphysiol.00298.2015. Epub 2015 Jun 11. PMID: 26066826.

57. Inscho EW, Imig JD, Cook AK, Pollock DM. ETA and ETB receptors differentially modulate afferent and efferent arteriolar responses to endothelin. Br J Pharmacol. 2005 Dec;146(7):1019-26. doi: 10.1038/sj.bjp.0706412. PMID: 16231007; PMCID: PMC1751231.

58. Kaszaki J, Érces D, Varga G, Szabó A, Vécsei L, Boros M. Kynurenines and intestinal neurotransmission: the role of N-methyl-D-aspartate receptors. J Neural Transm (Vienna). 2012 Feb;119(2):211-23. doi: 10.1007/s00702-011-0658-x. Epub 2011 May 27. PMID: 21617892.

59. Kiss C, Vécsei L, Kynurenines in the Brain: Preclinical and Clinical Studies, Therapeutic Considerations. In: Lajtha A., Banik N., Ray S.K. (eds) Handbook of Neurochemistry and Molecular Neurobiology. Springer, Boston, MA. 2009 https://doi: 10.1007/978-0-387-30375-8_5

60. Knyihar-Csillik E, Mihaly A, Krisztin-Peva B, Robotka H, Szatmari I, Fulop F, Toldi J, Csillik B, Vecsei L. The kynurenate analog SZR-72 prevents the nitroglycerol-induced increase of c-fos immunoreactivity in the rat caudal trigeminal nucleus: comparative studies of the effects of SZR-72 and kynurenic acid. Neurosci Res. 2008 Aug;61(4):429-32. doi: 10.1016/j.neures.2008.04.009. Epub 2008 May 2. PMID: 18541319.

61. Krumschnabel G, Eigentler A, Fasching M, Gnaiger E. Use of safranin for the assessment of mitochondrial membrane potential by high-resolution respirometry and fluorometry. Methods Enzymol. 2014;542:163-81. doi: 10.1016/B978-0-12-416618-9.00009-1. PMID: 24862266.

62. Levy MM, Fink MP, Marshall JC, Abraham E, Angus D, Cook D, Cohen J, Opal SM, Vincent JL, Ramsay G; International Sepsis Definitions Conference. 2001 SCCM/ESICM/ACCP/ATS/SIS International Sepsis Definitions Conference. Intensive Care Med. 2003 Apr;29(4):530-8. doi: 10.1007/s00134-003-1662-x. Epub 2003 Mar 28. PMID: 12664219.

63. Lewis AJ, Seymour CW, Rosengart MR. Current Murine Models of Sepsis. Surg Infect (Larchmt). 2016 Aug;17(4):385-93. doi: 10.1089/sur.2016.021. Epub 2016 Jun 15. PMID: 27305321; PMCID: PMC4960474.

64. López A, Lorente JA, Steingrub J, Bakker J, McLuckie A, Willatts S, Brockway M, Anzueto A, Holzapfel L, Breen D, Silverman MS, Takala J, Donaldson J, Arneson C, Grove G, Grossman S, Grover R. Multiple-center, randomized, placebo-controlled, double-blind study of the nitric oxide synthase inhibitor 546C88: effect on survival in patients with septic shock. Crit Care Med. 2004 Jan;32(1):21-30. doi: 10.1097/01.CCM.0000105581.01815.C6. PMID: 14707556.

65. Lukács M, Warfvinge K, Tajti J, Fülöp F, Toldi J, Vécsei L, Edvinsson L. Topical dura mater application of CFA induces enhanced expression of c-fos and glutamate in rat trigeminal nucleus caudalis: attenuated by KYNA derivate (SZR72). J Headache Pain. 2017 Dec;18(1):39. doi: 10.1186/s10194-017-0746-x. Epub 2017 Mar 23. PMID: 28337634; PMCID: PMC5364126.

66. Massey MJ, Shapiro NI. A guide to human in vivo microcirculatory flow image analysis. Crit Care. 2016 Feb 10;20:35. doi: 10.1186/s13054-016-1213-9. PMID: 26861691; PMCID: PMC4748457.

67. Matsuura T, Yukimura T, Kim S, Miura K, Iwao H. Selective blockade of endothelin receptor subtypes on systemic and renal vascular responses to endothelin-1 and IRL1620, a selective endothelin ETB-receptor agonist, in anesthetized rats. Jpn J Pharmacol. 1996 Jul;71(3):213-22. doi: 10.1254/jjp.71.213. PMID: 8854203.

68. Mándi Y, Endrész V, Mosolygó T, Burián K, Lantos I, Fülöp F, Szatmári I, Lőrinczi B, Balog A, Vécsei L. The Opposite Effects of Kynurenic Acid and Different Kynurenic Acid Analogs on Tumor Necrosis Factor-α (TNF-α) Production and Tumor Necrosis Factor-Stimulated Gene-6 (TSG-6) Expression. Front Immunol. 2019 Jun 21;10:1406. doi: 10.3389/fimmu.2019.01406. PMID: 31316502; PMCID: PMC6611419.

69. McMurdo L, Thiemermann C, Vane JR. The endothelin ETB receptor agonist, IRL 1620, causes vasodilatation and inhibits ex vivo platelet aggregation in the anaesthetised rabbit. Eur J Pharmacol. 1994 Jun 23;259(1):51-5. doi: 10.1016/0014-2999(94)90156-2. PMID: 7957593.

70. Mecs L, Tuboly G, Nagy E, Benedek G, Horvath G. The peripheral antinociceptive effects of endomorphin-1 and kynurenic acid in the rat inflamed joint model. Anesth Analg. 2009 Oct;109(4):1297-304. doi: 10.1213/ane.0b013e3181b21c5e. PMID: 19762760.

71. Mettler J, Simcock M, Sendi P, Widmer AF, Bingisser R, Battegay M, Fluckiger U, Bassetti S. Empirical use of antibiotics and adjustment of empirical antibiotic therapies in a university hospital: a prospective observational study. BMC Infect Dis. 2007 Mar 26;7:21. doi: 10.1186/1471-2334-7-21. PMID: 17386104; PMCID: PMC1847433.

72. Mino N, Kobayashi M, Nakajima A, Amano H, Shimamoto K, Ishikawa K, Watanabe K, Nishikibe M, Yano M, Ikemoto F. Protective effect of a selective endothelin receptor antagonist, BQ-123, in ischemic acute renal failure in rats. Eur J Pharmacol. 1992 Oct 6;221(1):77-83. doi: 10.1016/0014-2999(92)90774-x. PMID: 1459192.

73. Moore JP, Dyson A, Singer M, Fraser J. Microcirculatory dysfunction and resuscitation: why, when, and how. Br J Anaesth. 2015 Sep;115(3):366-75. doi: 10.1093/bja/aev163. PMID: 26269467.

74. Moullan N, Mouchiroud L, Wang X, Ryu D, Williams EG, Mottis A, Jovaisaite V, Frochaux MV, Quiros PM, Deplancke B, Houtkooper RH, Auwerx J. Tetracyclines Disturb Mitochondrial Function across Eukaryotic Models: A Call for Caution in Biomedical Research. Cell Rep. 2015 Mar 17;10(10):1681-1691. doi: 10.1016/j.celrep.2015.02.034. Epub 2015 Mar 12. PMID: 25772356; PMCID: PMC4565776.

75. Murando F, Peloso A, Cobianchi L. Experimental Abdominal Sepsis: Sticking to an Awkward but Still Useful Translational Model. Mediators Inflamm. 2019 Dec 5;2019:8971036. doi: 10.1155/2019/8971036. PMID: 31885502; PMCID: PMC6915118.

76. Nakahira K, Hisata S, Choi AM. The Roles of Mitochondrial Damage-Associated Molecular Patterns in Diseases. Antioxid Redox Signal. 2015 Dec 10;23(17):1329-50. doi: 10.1089/ars.2015.6407. Epub 2015 Aug 17. PMID: 26067258; PMCID: PMC4685486.

77. Nászai A, Terhes E, Kaszaki J, Boros M, Juhász L. Ca(2+)N It Be Measured? Detection of Extramitochondrial Calcium Movement With High-Resolution FluoRespirometry. Sci Rep. 2019 Dec 17;9(1):19229. doi: 10.1038/s41598-019-55618-5. PMID: 31848391; PMCID: PMC6917783.

78. Nemzek JA, Hugunin KM, Opp MR. Modeling sepsis in the laboratory: merging sound science with animal well-being. Comp Med. 2008 Apr;58(2):120-8. PMID: 18524169; PMCID: PMC2703167.

79. Nesterov SV, Skorobogatova YA, Panteleeva AA, Pavlik LL, Mikheeva IB, Yaguzhinsky LS, Nartsissov YR. NMDA and GABA receptor presence in rat heart mitochondria. Chem Biol Interact. 2018 Aug 1;291:40-46. doi: 10.1016/j.cbi.2018.06.004. Epub 2018 Jun 6. PMID: 29883723.

80. Osuchowski MF, Ayala A, Bahrami S, Bauer M, Boros M, Cavaillon JM, Chaudry IH, Coopersmith CM, Deutschman C, Drechsler S, Efron P, Frostell C, Fritsch G, Gozdzik W, Hellman J, Huber-Lang M, Inoue S, Knapp S, Kozlov AV, Libert C, Marshall JC, Moldawer LL, Radermacher P, Redl H, Remick DG, Singer M, Thiemermann C, Wang P, Wiersinga WJ, Xiao X, Zingarelli B. Minimum quality threshold in pre-clinical sepsis studies (MQTiPSS): an international expert consensus initiative for improvement of animal modeling in sepsis. Intensive Care Med Exp. 2018 Aug 14;6(1):26. doi: 10.1186/s40635-018-0189-y. PMID: 30112605; PMCID: PMC6093828.

81. Sengupta P. The Laboratory Rat: Relating Its Age With Human's. Int J Prev Med. 2013 Jun;4(6):624-30. PMID: 23930179; PMCID: PMC3733029.

82. Petros A, Bennett D, Vallance P. Effect of nitric oxide synthase inhibitors on hypotension in patients with septic shock. Lancet. 1991 Dec 21-28;338(8782-8783):1557-8. doi: 10.1016/0140-6736(91)92376-d. PMID: 1720856.

83. Piechota-Polanczyk A, Kleniewska P, Gorąca A. The influence of ETA and ETB receptor blockers on LPS-induced oxidative stress and NF-κB signaling pathway in heart. Gen Physiol Biophys. 2012 Sep;31(3):271-8. doi: 10.4149/gpb_2012_031. PMID: 23047940.

84. Pittet JF, Morel DR, Hemsen A, Gunning K, Lacroix JS, Suter PM, Lundberg JM. Elevated plasma endothelin-1 concentrations are associated with the severity of illness in patients with sepsis. Ann Surg. 1991 Mar;213(3):261-4. doi: 10.1097/00000658-199103000-00014. PMID: 1998407; PMCID: PMC1358338.

85. Pool R, Gomez H, Kellum JA. Mechanisms of Organ Dysfunction in Sepsis. Crit Care Clin. 2018 Jan;34(1):63-80. doi: 10.1016/j.ccc.2017.08.003. Epub 2017 Oct 18. PMID: 29149942; PMCID: PMC6922007.

86. Pundir M, Arora S, Kaur T, Singh R, Singh AP. Effect of modulating the allosteric sites of N-methyl-D-aspartate receptors in ischemia-reperfusion induced acute kidney injury. J Surg Res. 2013 Aug;183(2):668-77. doi: 10.1016/j.jss.2013.01.040. Epub 2013 Feb 10. PMID: 23498342.

87. Qiu P, Cui X, Barochia A, Li Y, Natanson C, Eichacker PQ. The evolving experience with therapeutic TNF inhibition in sepsis: considering the potential influence of risk of death. Expert Opin Investig Drugs. 2011 Nov;20(11):1555-64. doi: 10.1517/13543784.2011.623125. Epub 2011 Oct 1. PMID: 21961576; PMCID: PMC3523300.

88. Rademann P, Weidinger A, Drechsler S, Meszaros A, Zipperle J, Jafarmadar M, Dumitrescu S, Hacobian A, Ungelenk L, Röstel F, Kaszaki J, Szabo A, Skulachev VP, Bauer M, Bahrami S, Weis S, Kozlov AV, Osuchowski MF. Mitochondria-Targeted Antioxidants SkQ1 and MitoTEMPO Failed to Exert a Long-Term Beneficial Effect in Murine Polymicrobial Sepsis. Oxid Med Cell Longev. 2017;2017:6412682. doi: 10.1155/2017/6412682. Epub 2017 Sep 19. PMID: 29104729; PMCID: PMC5625755.

89. Rameau GA, Chiu LY, Ziff EB. Bidirectional regulation of neuronal nitric-oxide synthase phosphorylation at serine 847 by the N-methyl-D-aspartate receptor. J Biol Chem. 2004 Apr 2;279(14):14307-14. doi: 10.1074/jbc.M311103200. Epub 2004 Jan 13. PMID: 14722119.

90. Reinhart K, Daniels R, Kissoon N, Machado FR, Schachter RD, Finfer S. Recognizing Sepsis as a Global Health Priority - A WHO Resolution. N Engl J Med. 2017 Aug 3;377(5):414-417. doi: 10.1056/NEJMp1707170. Epub 2017 Jun 28. PMID: 28658587.

91. Reinhart K, Karzai W. Anti-tumor necrosis factor therapy in sepsis: update on clinical trials and lessons learned. Crit Care Med. 2001 Jul;29(7 Suppl):S121-5. doi: 10.1097/00003246-200107001-00037. PMID: 11445746.

92. Riedemann NC, Ward PA. Anti-inflammatory strategies for the treatment of sepsis. Expert Opin Biol Ther. 2003 Apr;3(2):339-50. doi: 10.1517/14712598.3.2.339. PMID: 12662146

93. Rittirsch D, Flierl MA, Ward PA. Harmful molecular mechanisms in sepsis. Nat Rev Immunol. 2008 Oct;8(10):776-87. doi: 10.1038/nri2402. PMID: 18802444; PMCID: PMC2786961.

94. Selin AA, Lobysheva NV, Nesterov SV, Skorobogatova YA, Byvshev IM, Pavlik LL, Mikheeva IB, Moshkov DA, Yaguzhinsky LS, Nartsissov YR. On the regulative role of the glutamate receptor in mitochondria. Biol Chem. 2016 May;397(5):445-58. doi: 10.1515/hsz-2015-0289. PMID: 26812870.

95. Singer M, Deutschman CS, Seymour CW, Shankar-Hari M, Annane D, Bauer M, Bellomo R, Bernard GR, Chiche JD, Coopersmith CM, Hotchkiss RS, Levy MM, Marshall JC, Martin GS, Opal SM, Rubenfeld GD, van der Poll T, Vincent JL, Angus DC. The Third International Consensus Definitions for Sepsis and Septic Shock (Sepsis-3). JAMA. 2016 Feb 23;315(8):801-10. doi: 10.1001/jama.2016.0287. PMID: 26903338; PMCID: PMC4968574.

96. Spronk PE, Kanoore-Edul VS, Ince C. "Microcirculatory and Mitochondrial Distress Syndrome (MMDS): A New Look at Sepsis," in *Functional Hemodynamic Monitoring* (Springer-Verlag), 47–67. doi:10.1007/3-540-26900-2_5

97. Szalay L, Kaszaki J, Nagy S, Boros M. The role of endothelin-1 in circulatory changes during hypodynamic sepsis in the rat. Shock. 1998 Aug;10(2):123-8. doi: 10.1097/00024382-199808000-00007. PMID: 9721979.

98. Tanaka M, Bohár Z, Vécsei L. Are Kynurenines Accomplices or Principal Villains in Dementia? Maintenance of Kynurenine Metabolism. Molecules. 2020 Jan 28;25(3):564. doi: 10.3390/molecules25030564. PMID: 32012948; PMCID: PMC7036975.

99. Tanaka T, Narazaki M, Kishimoto T. Immunotherapeutic implications of IL-6 blockade for cytokine storm. Immunotherapy. 2016 Jul;8(8):959-70. doi: 10.2217/imt-2016-0020. PMID: 27381687.

100. Taeb AM, Hooper MH, Marik PE. Sepsis: Current Definition, Pathophysiology, Diagnosis, and Management. Nutr Clin Pract. 2017 Jun;32(3):296-308. doi: 10.1177/0884533617695243. Epub 2017 Mar 17. PMID: 28537517.

101. Trásy D, Tánczos K, Németh M, Hankovszky P, Lovas A, Mikor A, László I, Hajdú E, Osztroluczki A, Fazakas J, Molnár Z; EProK study group. Early procalcitonin kinetics and appropriateness of empirical antimicrobial therapy in critically ill patients: A prospective observational study. J Crit Care. 2016 Aug;34:50-5. doi: 10.1016/j.jcrc.2016.04.007. Epub 2016 Apr 13. PMID: 27288610.

102. Trzeciak S, Glaspey LJ, Dellinger RP, Durflinger P, Anderson K, Dezfulian C, Roberts BW, Chansky ME, Parrillo JE, Hollenberg SM. Randomized controlled trial of inhaled nitric oxide for the treatment of microcirculatory dysfunction in patients with sepsis*. Crit Care Med. 2014 Dec;42(12):2482-92. doi: 10.1097/CCM.0000000000000549. PMID: 25080051.

103. Turski MP, Turska M, Paluszkiewicz P, Parada-Turska J, Oxenkrug GF. Kynurenic Acid in the digestive system-new facts, new challenges. Int J Tryptophan Res. 2013 Sep 4;6:47-55. doi: 10.4137/IJTR.S12536. PMID: 24049450; PMCID: PMC3772988.

104. Tykocki NR, Watts SW. The interdependence of endothelin-1 and calcium: a review. Clin Sci (Lond). 2010 Jul 23;119(9):361-72. doi: 10.1042/CS20100145. PMID: 20662769; PMCID: PMC3960801.

105. Varga G, Erces D, Fazekas B, Fülöp M, Kovács T, Kaszaki J, Fülöp F, Vécsei L, Boros M. N-Methyl-D-aspartate receptor antagonism decreases motility and inflammatory activation in the early phase of acute experimental colitis in the rat. Neurogastroenterol Motil. 2010 Feb;22(2):217-25, e68. doi: 10.1111/j.1365-2982.2009.01390.x. Epub 2009 Sep 3. PMID: 19735360.

106. Vécsei L, Szalárdy L, Fülöp F, Toldi J. Kynurenines in the: recent advances and new questions. Nat Rev Drug Discov. 2013 Jan;12(1):64-82. doi: 10.1038/nrd3793. Epub 2012 Dec 14. PMID: 23237916.

107. Vincent JL, Marshall JC, Namendys-Silva SA, François B, Martin-Loeches I, Lipman J, Reinhart K, Antonelli M, Pickkers P, Njimi H, Jimenez E, Sakr Y; ICON investigators. Assessment of the worldwide burden of critical illness: the intensive care over nations (ICON) audit. Lancet Respir Med. 2014 May;2(5):380-6. doi: 10.1016/S2213-2600(14)70061-X. Epub 2014 Apr 14. PMID: 24740011.

108. Vincent JL, Moreno R, Takala J, Willatts S, De Mendonça A, Bruining H, Reinhart CK, Suter PM, Thijs LG. The SOFA (Sepsis-related Organ Failure Assessment) score to describe organ dysfunction/failure. On behalf of the Working Group on Sepsis-Related Problems of the European Society of Intensive Care Medicine. Intensive Care Med. 1996 Jul;22(7):707-10. doi: 10.1007/BF01709751. PMID: 8844239.

109. Wang K, Xie S, Xiao K, Yan P, He W, Xie L. Biomarkers of Sepsis-Induced Acute Kidney Injury. Biomed Res Int. 2018 Apr 24;2018:6937947. doi: 10.1155/2018/6937947. PMID: 29854781; PMCID: PMC5941779.

110. Wang J, Simonavicius N, Wu X, Swaminath G, Reagan J, Tian H, Ling L. Kynurenic acid as a ligand for orphan G protein-coupled receptor GPR35. J Biol Chem. 2006 Aug 4;281(31):22021-8. doi: 10.1074/jbc.M603503200. Epub 2006 Jun 5. PMID: 16754668.

111. Walczak K, Wnorowski A, Turski WA, Plech T. Kynurenic acid and cancer: facts and controversies. Cell Mol Life Sci. 2020 Apr;77(8):1531-1550. doi: 10.1007/s00018-019-03332-w. Epub 2019 Oct 28. PMID: 31659416; PMCID: PMC7162828.

112. Wirthgen E, Hoeflich A, Rebl A, Günther J. Kynurenic Acid: The Janus-Faced Role of an Immunomodulatory Tryptophan Metabolite and Its Link to Pathological Conditions. Front Immunol. 2018 Jan 10;8:1957. doi: 10.3389/fimmu.2017.01957. PMID: 29379504; PMCID: PMC5770815.

113. Wolfárd A, Kaszaki J, Szabó C, Szalay L, Nagy S, Boros M. Prevention of early myocardial depression in hyperdynamic endotoxemia in dogs. Shock. 2000 Jan;13(1):46-51. doi: 10.1097/00024382-200013010-00009. PMID: 10638669.

114. Wolfárd A, Szalay L, Kaszaki J, Sahin-Tóth G, Vangel R, Balogh A, Boros M. Dynamic in vivo observation of villus microcirculation during small bowel autotransplantation: effects of endothelin-A receptor inhibition. Transplantation. 2002 May 15;73(9):1511-3. doi: 10.1097/00007890-200205150-00024. PMID: 12023633.

115. Yanagisawa M, Kurihara H, Kimura S, Tomobe Y, Kobayashi M, Mitsui Y, Yazaki Y, Goto K, Masaki T. A novel potent vasoconstrictor peptide produced by vascular endothelial cells. Nature. 1988 Mar 31;332(6163):411-5. doi: 10.1038/332411a0. PMID: 2451132.

116. Yetkin-Arik B, Vogels IMC, Nowak-Sliwinska P, Weiss A, Houtkooper RH, Van Noorden CJF, Klaassen I, Schlingemann RO. The role of glycolysis and mitochondrial respiration in the formation and functioning of endothelial tip cells during angiogenesis. Sci Rep. 2019 Aug 30;9(1):12608. doi: 10.1038/s41598-019-48676-2. PMID: 31471554; PMCID: PMC6717205.

117. Yuki K, Suzuki T, Katoh S, Kakinuma Y, Miyauchi T, Mitsui Y. Endothelin-1 stimulates cardiomyocyte injury during mitochondrial dysfunction in culture. Eur J Pharmacol. 2001 Nov 16;431(2):163-70. doi: 10.1016/s0014-2999(01)01434-0. PMID: 11728422.

118. Zhai X, Yang Z, Zheng G, Yu T, Wang P, Liu X, Ling Q, Jiang L, Tang W. Lactate as a Potential Biomarker of Sepsis in a Rat Cecal Ligation and Puncture Model. Mediators Inflamm. 2018 Mar 7;2018:8352727. doi: 10.1155/2018/8352727. PMID: 29706801; PMCID: PMC5863333.

119. Zhang H, Feng YW, Yao YM. Potential therapy strategy: targeting mitochondrial dysfunction in sepsis. Mil Med Res. 2018 Nov 26;5(1):41. doi: 10.1186/s40779-018-0187-0. PMID: 30474573; PMCID: PMC6260865.

120. Zhe Z, Hongyuan B, Wenjuan Q, Peng W, Xiaowei L, Yan G. Blockade of glutamate receptor ameliorates lipopolysaccharide-induced sepsis through regulation of neuropeptides. Biosci Rep. 2018 May 8;38(3):BSR20171629. doi: 10.1042/BSR20171629. PMID: 29440461; PMCID: PMC5938426.

121. Zorova LD, Popkov VA, Plotnikov EY, Silachev DN, Pevzner IB, Jankauskas SS, Babenko VA, Zorov SD, Balakireva AV, Juhaszova M, Sollott SJ, Zorov DB. Mitochondrial membrane potential. Anal Biochem. 2018 Jul 1;552:50-59. doi: 10.1016/j.ab.2017.07.009. Epub 2017 Jul 12. PMID: 28711444; PMCID: PMC5792320.

9. ANNEX

I. Rutai A, Fejes R, Juhász L, Tallósy SP, Poles MZ, Földesi I, Mészáros AT, Szabó A, Boros M, Kaszaki J. Endothelin A and B Receptors: Potential Targets for Microcirculatory-Mitochondrial Therapy in Experimental Sepsis. Shock. 2020 Jul;54(1):87-95. doi: 10.1097/SHK.0000000000001414. PMID: 31318833.

II. Juhász L, Rutai A, Fejes R, Tallósy SP, Poles MZ, Szabó A, Szatmári I, Fülöp F, Vécsei L, Boros M, Kaszaki J. Divergent Effects of the N-Methyl-D-Aspartate Receptor Antagonist Kynurenic Acid and the Synthetic Analog SZR-72 on Microcirculatory and Mitochondrial Dysfunction in Experimental Sepsis. Front Med (Lausanne). 2020 Nov 27;7:566582. doi: 10.3389/fmed.2020.566582. PMID: 33330526; PMCID: PMC7729001